

6.0 RE-USABLE SOLID ROCKET MOTOR

All Reusable Solid Rocket Motor (RSRM) investigation fault tree legs have been closed for the STS-107 RSRM set, RSRM-88. All Contract End Item (CEI) performance specifications were met including all flight individual and paired motor requirements. Postflight inspections revealed a tear in the right-hand nozzle flex boot that is considered an IFA (STS-107-M-01), but the tear is attributed to thrust tail-off or splashdown events. A slightly low out-of-family thrust level was observed for the right-hand motor in the 113.5 to 114.5 second interval during thrust tail-off, but the resultant thrust imbalance was still within family experience and CEI limits. The new experience has been reviewed and accepted as being within the statistical expectations for the RSRM motor population and is attributed to the increased population sample size (see Section 3.4 for more details).

7.0 SOLID ROCKET BOOSTER

The Solid Rocket Booster (SRB) fault tree for the STS-107 SRB set, SRB BI116, remains open due to possible debris sources at the forward SRB/External Tank (ET) separation bolt catcher assembly and the forward Booster Separation Motors (BSM). The STS-107 SRBs performed nominally and there were no reported SRB IFAs.

Four blocks on the STS-107 SRB fault tree remain open pending completion of forward bolt catcher testing. The bolt catcher, shown in Figure 7-1, was not qualified as an assembly, and structural qualification testing was not representative of the current flight configuration. The exact magnitude of loads transmitted to the bolt catcher housing cannot be determined based on available data. The SLA-561 thermal protection system (TPS) material on the bolt catcher was qualified by test and analysis for general ET application, but no pyrotechnic shock testing was performed. There is no test data available on the bolt catcher honeycomb dynamic crush strength versus separation bolt velocity, and random pressure loading from the NASA Standard Initiator (NSI) ejection was not included in the original qualification tests. Lastly, the running torque/break-away torque was not measured during STS-107 bolt catcher fastener and ET range safety system (RSS) fairing installation, which is used to verify the insert locking feature is in place. A review has determined that the bolt catchers and RSS fairings were installed and secured for flight with the correct bolts and final torque. Testing is in work to close the four remaining fault tree blocks, but initial static tests results show failure below the required safety factor of 1.4.

Two other blocks on the STS-107 SRB fault tree remain open that pertain to potential debris from the forward BSMs. Inspection of the forward BSMs found no indication of unburned propellant or any indication that the BSMs contained any Foreign Object Debris (FOD). The two debris related fault tree blocks will remain open pending transport and impact analysis.

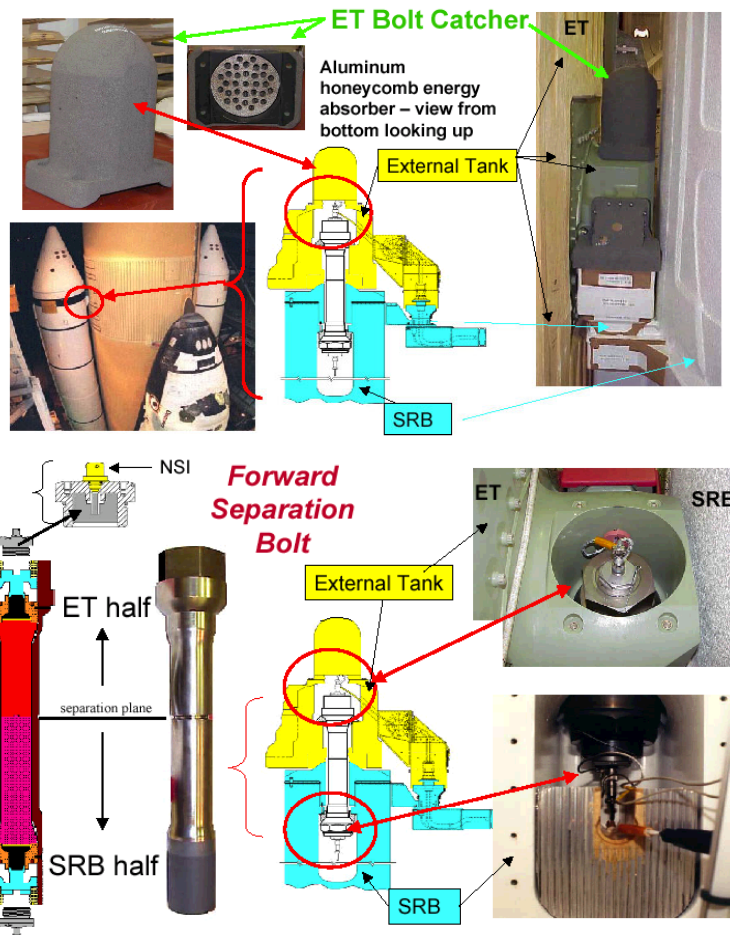


Figure 7-1. Details of SRB/ET forward separation bolt catcher assembly

8.0 SPACE SHUTTLE MAIN ENGINE

All Space Shuttle Main Engine (SSME) investigation fault tree legs have been closed. The STS-107 Block II SSMEs (center #2055, left #2053, and right #2049) performed nominally and there were no reported SSME In-Flight Anomalies (IFAs).

9.0 ENVIRONMENTAL FACTORS

9.1 INTRODUCTION

A survey was conducted of the relevant environmental factors during STS-107/ET-93 processing to determine if a correlation could be drawn between those factors and ET bipod foam loss observed in flight. The data are inconclusive as to whether any correlation can be shown between environmental factors and ET bipod foam loss. The review considered ET age and exposure time, as well as weather factors such as rainfall, temperature, and humidity.

9.2 AGE AND EXPOSURE

The ET age was compared for various flights, presented in Figure 9-1. As shown in Figure 9-2, the ET age for STS-107/ET-93, 806 days, falls above the 95% confidence interval upper limit for the average age of all tanks, mean value 689 days, as well as the average age for all tanks with known bipod foam loss. STS-107/ET-93 also falls within the 95% confidence limit for missions with known bipod foam loss. Although the upper bound of the 95% confidence interval of the age of missions with bipod foam loss appears to be greater than the other groups in Figure 9-2, the 95% confidence interval limits of the different groups overlap each other. Therefore, data are inconclusive as to whether a correlation can be drawn about ET age and bipod foam loss.

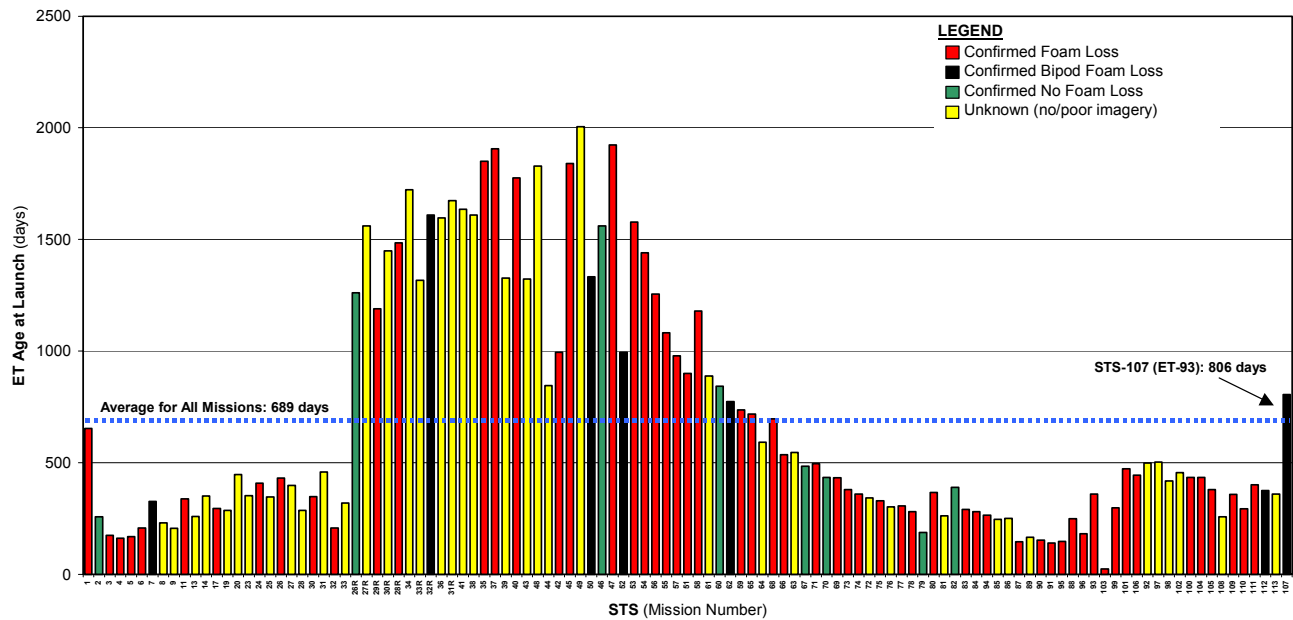


Figure 9-1. ET age for all STS missions

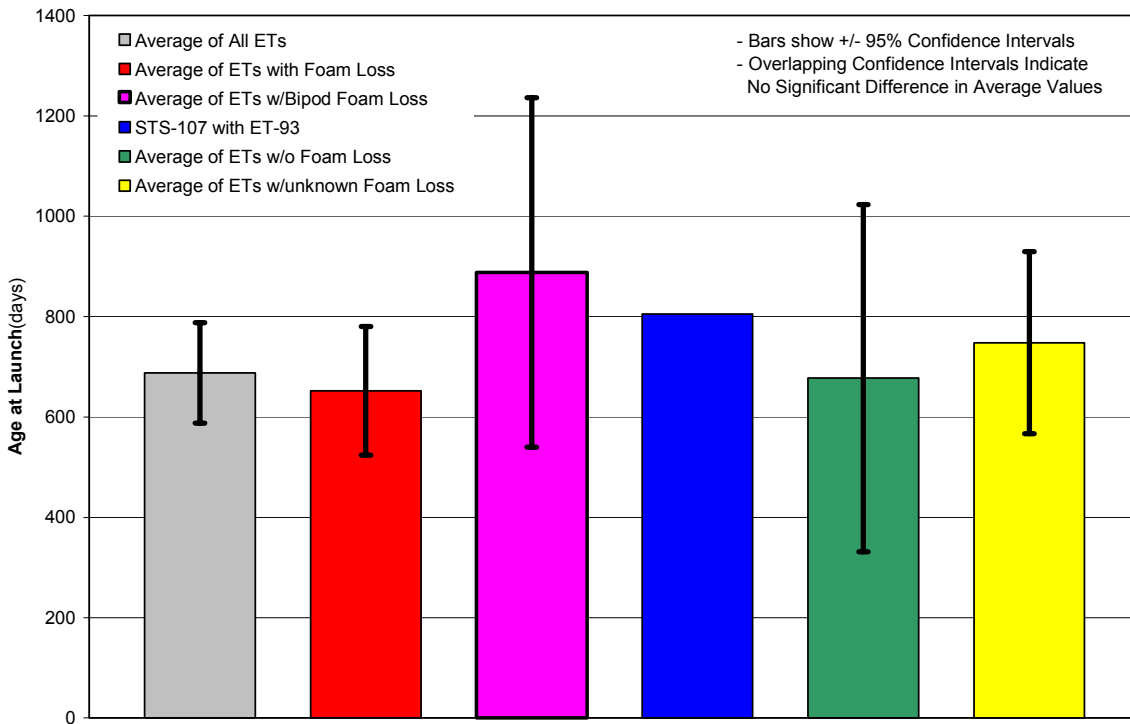


Figure 9-2. ET age for STS-107 compared to ET age for missions with and without bipod foam loss

A similar comparison was made relating ET exposure time and bipod foam loss across the flight history, shown in Figure 9-3. Note that the STS-107/ET-93 exposure time, 39 days, is the same as the mean value for all STS flights. As shown in Figure 9-4, the STS-107/ET-93 exposure time falls within the 95% confidence limit of all missions' ET exposure time, as well as the time confidence limits for flights with or without known bipod foam loss. The STS-107/ET-93 exposure time is larger than the 95% confidence upper bound for missions with known bipod foam loss. However, as stated above when discussing ET age, the 95% confidence limits of the different groups in Figure 9-4 overlap each other, and data are inconclusive as to whether ET exposure time and bipod foam loss can be correlated.

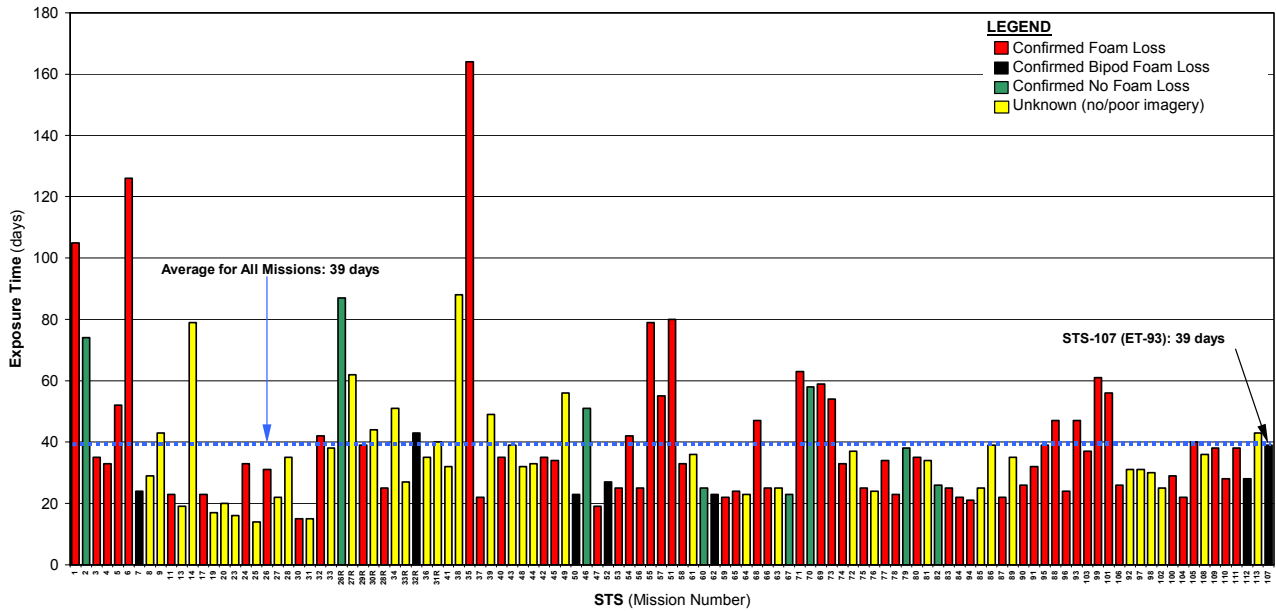


Figure 9-3. ET exposure time (to weather) prelaunch for all STS missions

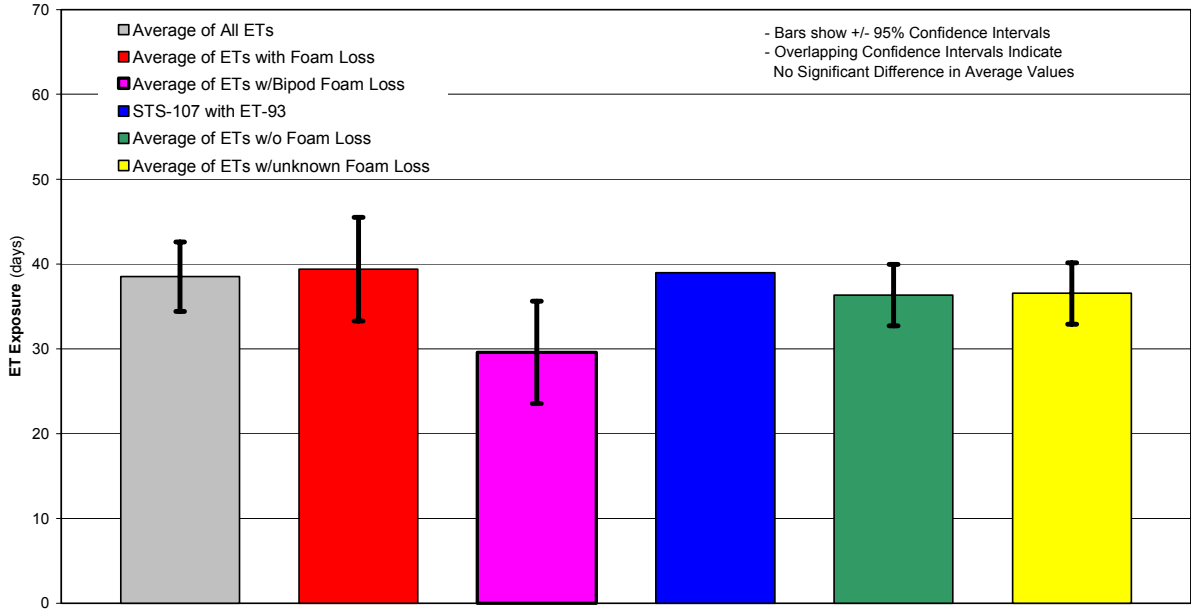


Figure 9-4. ET exposure time (to weather) for STS-107 compared to ET exposure time for missions with and without bipod foam loss

9.3 WEATHER FACTORS

An extensive review of the relevant weather at Kennedy Space Center (KSC) was conducted in order to determine if a correlation could be derived for the weather conditions impact on ET bipod foam loss. The precipitation review examined total rainfall, maximum one-day rainfall, average daily rainfall, launch day rainfall, and L-5 days through liftoff total rainfall. Figure 9-5 shows the total prelaunch rainfall for all STS missions. As shown in Figure 9-6, although the STS-107 value for total prelaunch rainfall, 12.78 inches, is greater than the mean value for all mission, 5.45 inches, the data are inconclusive as to whether a correlation can be made for ET bipod foam loss as a function of total rainfall prelaunch. The 95% confidence limit of the missions with ET bipod foam loss overlaps the confidence interval for all missions, as well as missions with no foam loss.

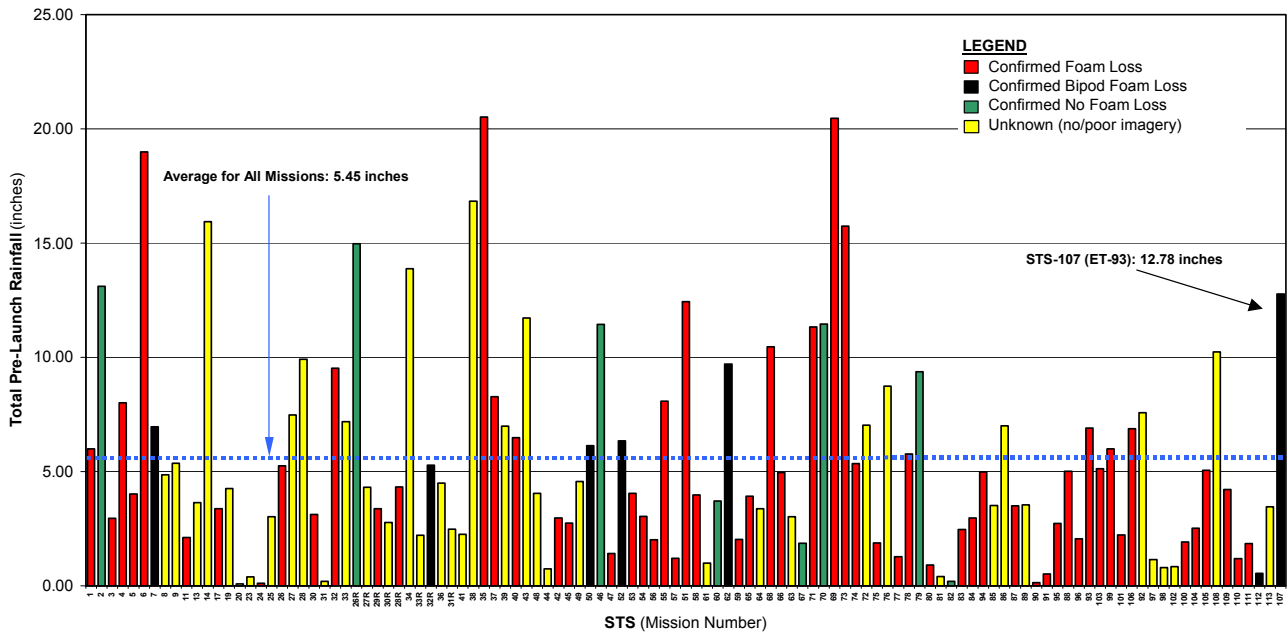


Figure 9-5. Total prelaunch rainfall for all STS missions

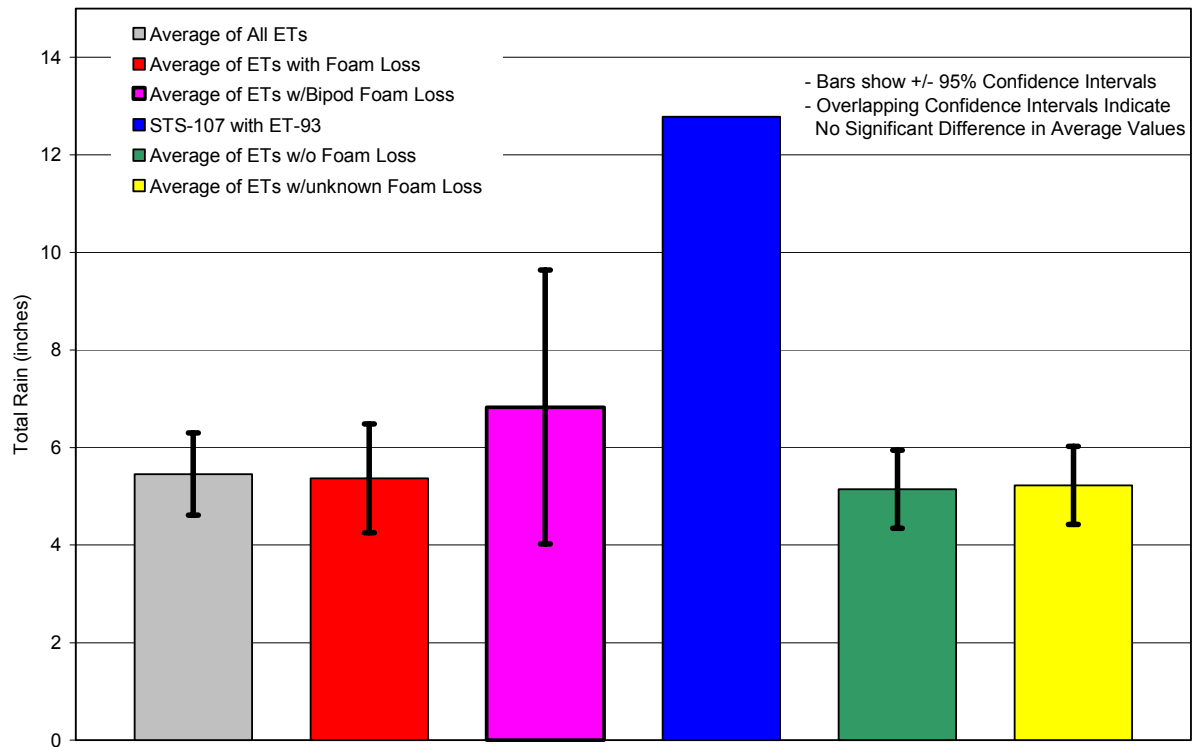


Figure 9-6. Total rainfall for STS-107 compared to total rainfall for missions with and without bipod foam loss

Similarly, the other rainfall parameters studied (e.g., average daily, day-of-launch) reveal no correlations for ET bipod foam loss. Figure 9-7 and Figure 9-8 show the data correlation for average daily prelaunch rainfall. The STS-107 value, 0.33 inches, and the mean value for missions with bipod foam loss are greater than the average mission value, 0.14 inches. However, the confidence intervals overlap each other, and the data are inconclusive as to whether average daily rainfall and ET bipod foam loss can be correlated.

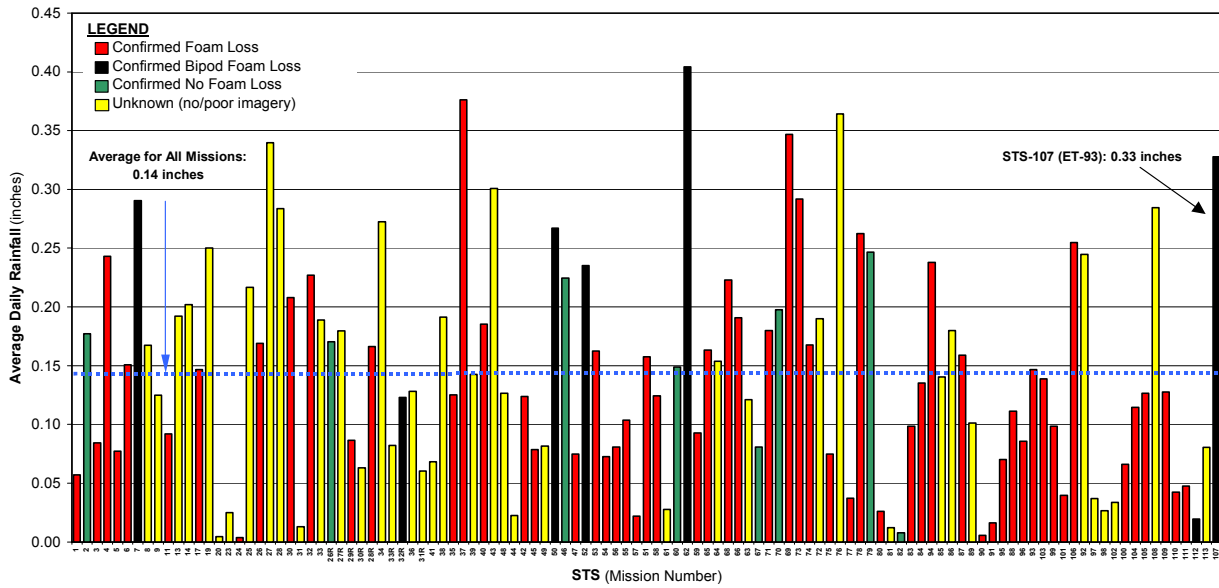


Figure 9-7. Average daily rainfall prelaunch for all STS missions

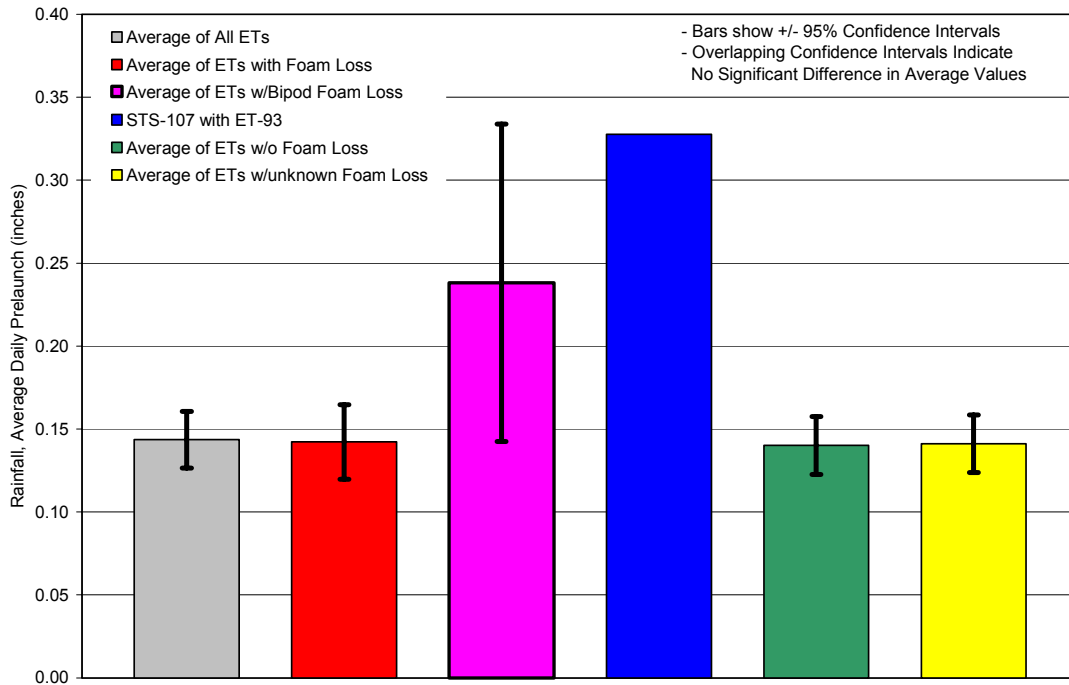


Figure 9-8. Average daily rainfall prelaunch for STS-107 compared to average daily rainfall for missions with and without bipod foam loss

In addition to rainfall, the study also reviewed average, minimum, and maximum temperature, dew point, and humidity for both prelaunch and day of launch. Figure 9-9 shows the day-of-launch average temperature. The STS-107 day-of-launch average temperature, 58 °F, was less than the mean value for all missions, 71 °F, but no correlation can be made between day-of-launch average temperature and ET bipod foam loss. Similar comparisons made for other temperature samplings, dew point (Figure 9-10), and humidity (Figure 9-11), yielded no correlations either.

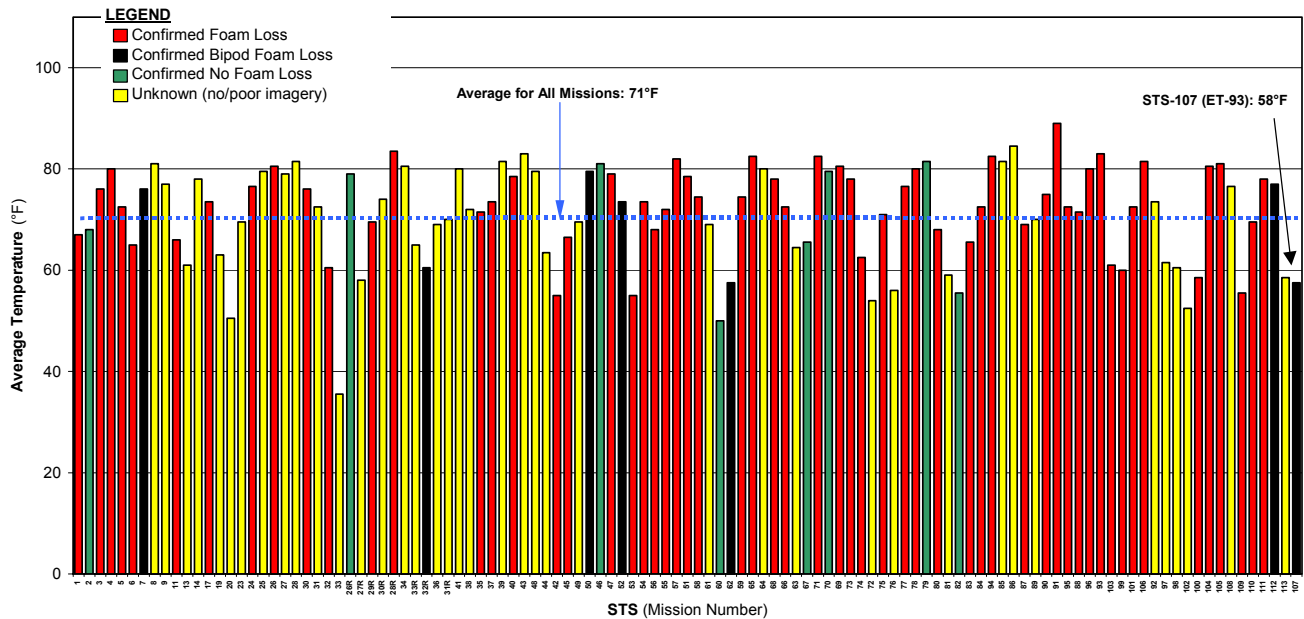


Figure 9-9. Day-of-launch average temperature for all STS missions

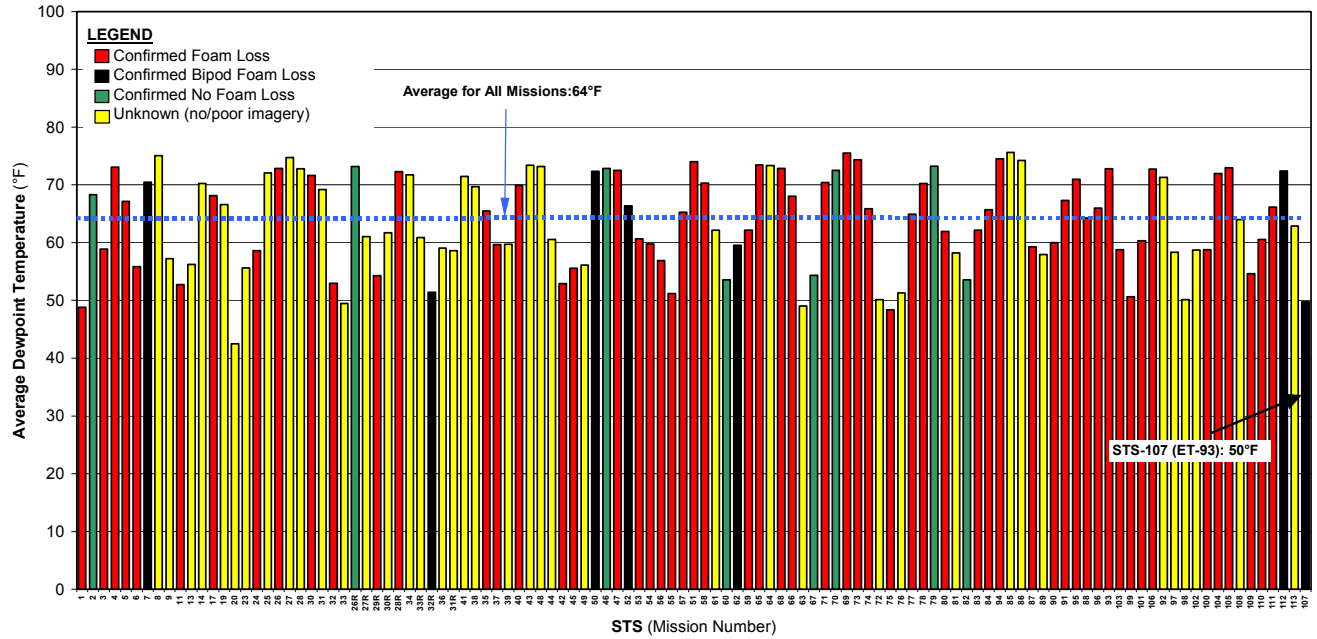


Figure 9-10. Prelaunch average dewpoint for all STS missions

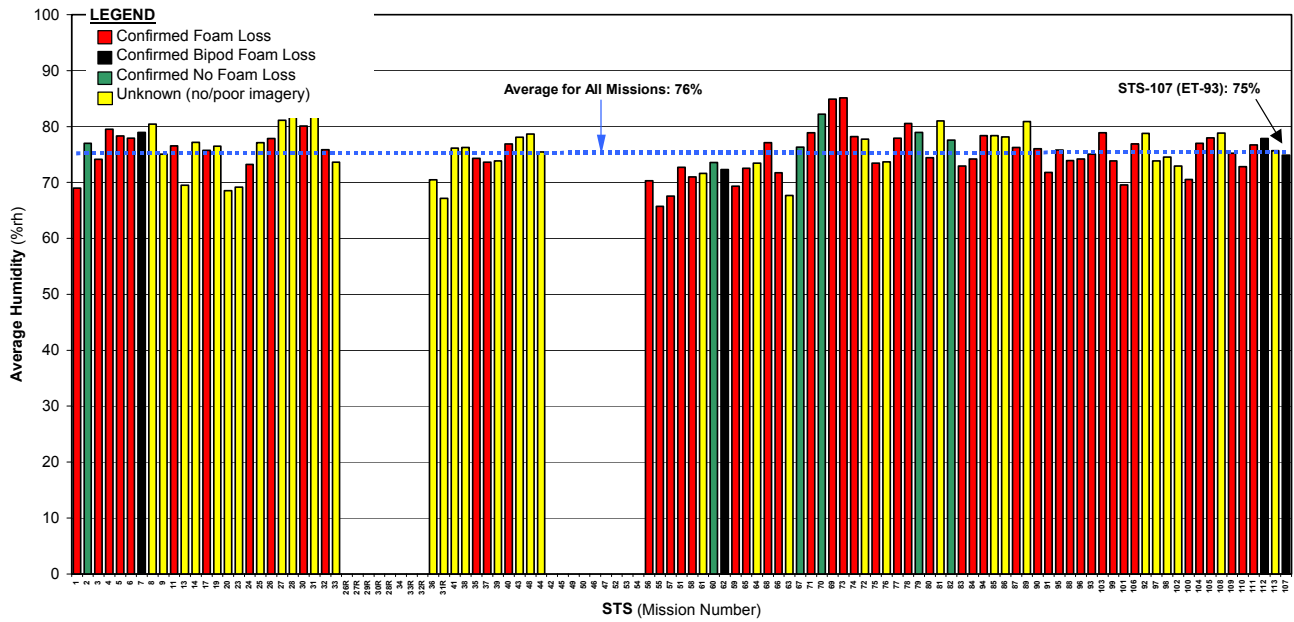


Figure 9-11. Prelaunch average humidity for all STS missions

10.0 LEFT WING PROCESSING AND RCC DESIGN

10.1 INTRODUCTION

This section summarizes the processing effort performed on the left wing of the Space Shuttle Columbia from the last Orbiter Major Maintenance (OMM) period through the launch of STS-107, and provides some background on the design of the RCC panels used on the orbiter. The processing includes all work done on Columbia from the major maintenance period (Columbia J3-OMM) through the flight of the STS-109 mission and all the normal preflight work done in preparation for the STS-107 mission.

10.2 LEFT WING PROCESSING (PALMDALE, J3-OMM)

Columbia was in Palmdale, California, for its most recent OMM from September 1999 through March 2001. The work performed on the left wing included work on the electrical power and distribution system, instrumentation, mechanisms, structures, and the Thermal Protection System (TPS). There were 29 Problem Reports (PRs) on the electrical system, mostly wire lead discrepancies and wire stow issues. Two pyrotechnic connectors were found out of configuration and repaired. Instrumentation sensors and wire splices accounted for 20 PRs on the left wing and all were appropriately resolved. In the mechanisms area, a main landing gear door rotational pin inspection was partially performed at Palmdale and subsequently completed at the KSC. Slight damage to the chromium plating of the forward inboard gear door hook was repaired. The gear downlock bungee was sent to the vendor for refurbishment.

Palmdale logged 62 PRs to the left wing structure that addressed elevon cove corrosion, elevon flipper door modification (material change from Inconel to Aluminum), and minor work on the main landing gear door.

All Reinforced Carbon-Carbon (RCC) upper and lower wing Leading Edge Structural Subsystem (LESS) access panels, spar insulators, ear muff insulators, wing leading edge RCC panels, and spar fittings (see Figure 10-1 and Figure 10-2) were removed and inspected for discoloration and damage. Visual pinhole inspections were performed on each RCC panel and the wing leading edge spar was inspected for damage. Oversized pinholes were originally reported in RCC panels 8 and 19, but after further evaluation with an optical comparator, it was determined that the pinholes were acceptable. No other significant damage was noted. Leading edge RCC panels 6 and 13 through 17 were sent to the vendor (Vought) for refurbishment. New shims were installed to accommodate the reinstallation of the spar insulators.

The panels and spar fittings were reinstalled and all step and gap measurements were taken. At that time, gaps were found to be unacceptable in numerous locations. Wing leading edge RCC panels 11, 12, 17, and 18 were removed and additional anomalies were noted, which included insufficient step and gap, spar fitting shims not per design (too small), and the lower access panel nutplates debonded and/or with low running torque. The low torque was due to a combination of the shim problem and a procedural error on the torque sequence. All 22 RCC panels were removed a second time. The

nutplate issues were resolved by removing and replacing the nutplates that were accessible and securing with safety wire those that were not accessible. All anomalies identified were repaired, reworked, or accepted by Material Review (MR).

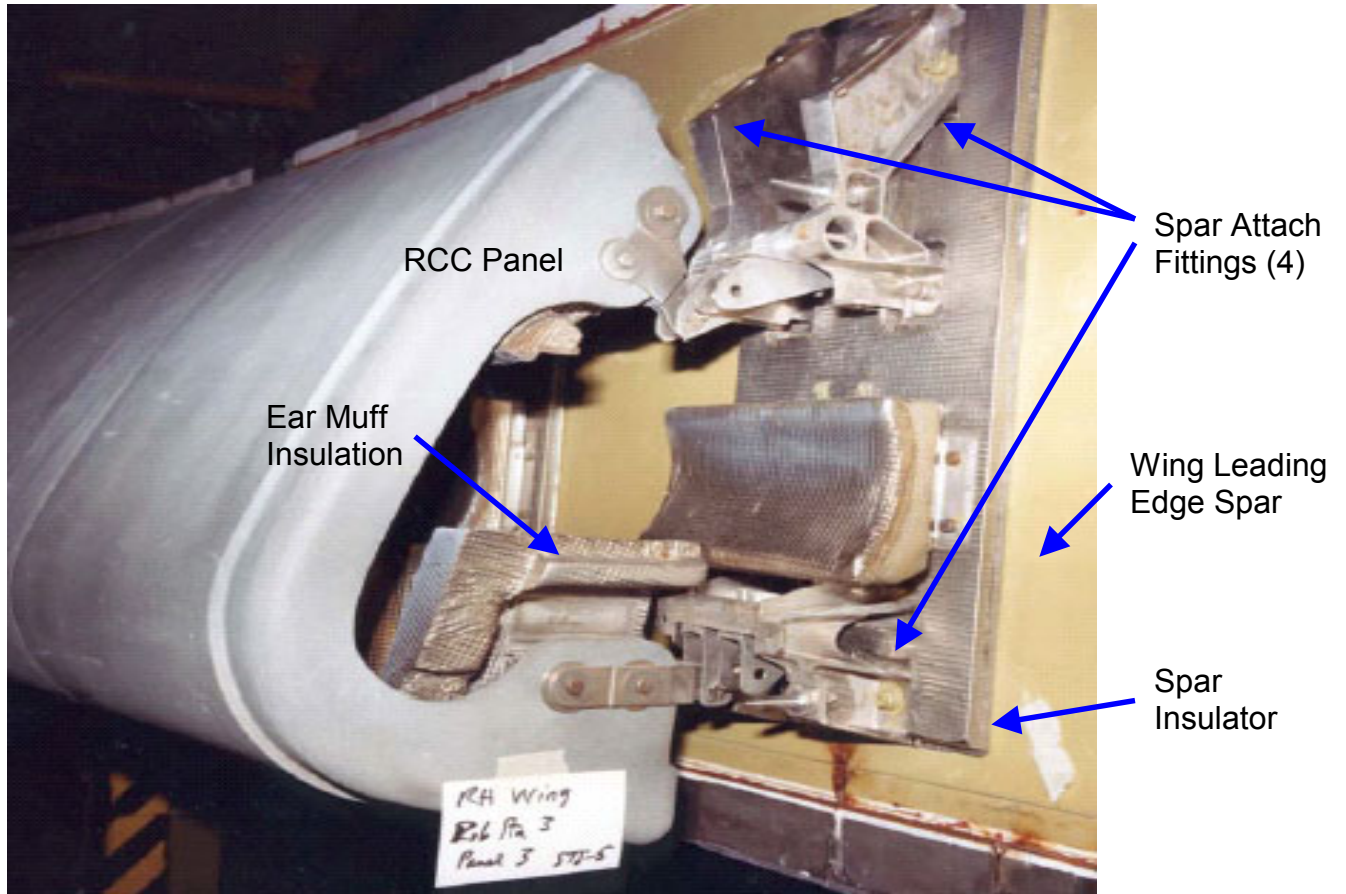


Figure 10-1. RCC components

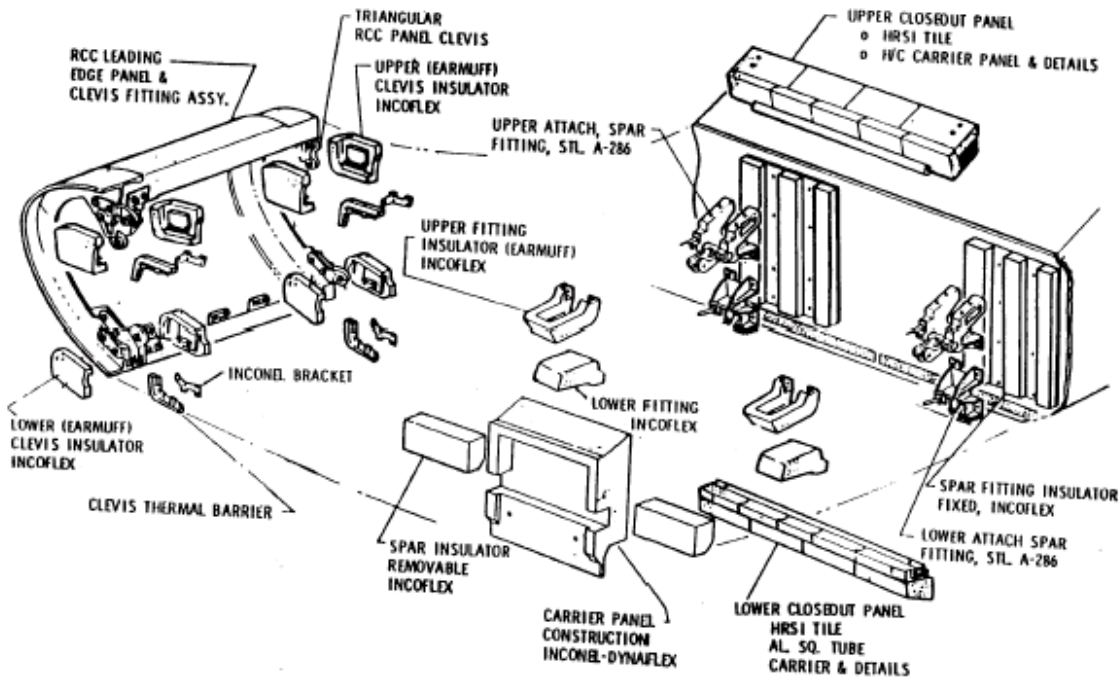


Figure 10-2. RCC panel assembly

Tiles are attached to a strain isolation pad and then to the orbiter structure by a Room Temperature Vulcanized (RTV) adhesive. The outer tile surfaces must be flush with one another to preclude steps that would lead to excessive heat damage of surrounding tiles due to aerodynamic heating (Figure 10-3). Gaps present between adjacent tiles must be adequately sealed. There were 200 tile PRs worked for step and gap, gap fillers, and repair on the elevon cove area tile. One hundred thirty one (131) upper and lower wing surface tiles were replaced for various reasons, including baseline removal and replacements, damaged tile, instrumentation problems, and structural inspections. Wear and tear accounted for 27 maintenance items. Tile gap filler replacements numbered 58 with no issues noted. There were 100 discrepancy reports for minor tile putty repairs. Six chits (change items) were worked on the left side, mostly in the landing gear area. The main landing gear rotational pins, wheel well wire, and landing gear structural components were all inspected. The left inboard brake interference was slightly out of tolerance, but was corrected. One chit addressed the application of corrosion protection coating to the forward wing spar.

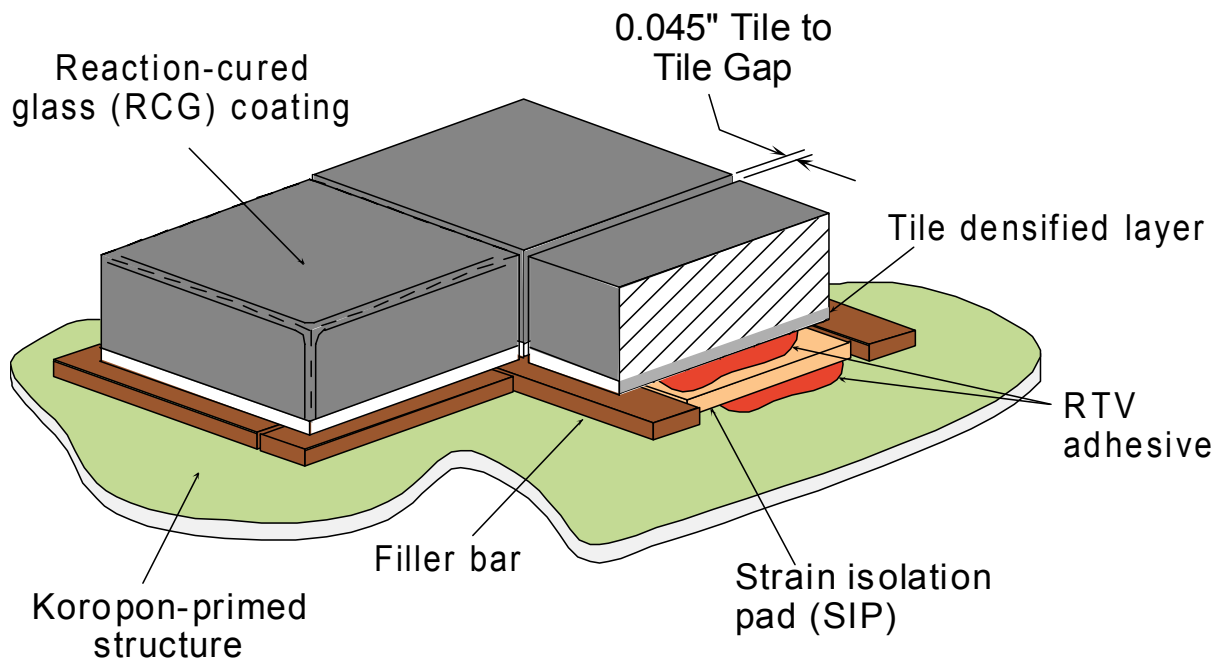


Figure 10-3. Typical tile installation

Twenty Master Change Records were incorporated during the period. They included the replacement of the aluminized Mylar tape that lines the wheel well walls, the deletion of some non-functional acoustic sensors, and the removal of inactive Modular Auxiliary Data System (MADS) instrumentation. An additional part of that effort was the modification of the elevon columbium seal springs, some wing leading edge protective shielding, and enhancements to various gap fillers.

The 22 left wing Line Replaceable Units (LRUs) that were replaced included the RCC panels previously mentioned, a hydraulic retract valve, the landing gear extend isolation valve, left main landing gear bungee, Tee seals, and an Inconel (Incoflex) insulator.

All items not completed at Palmdale were dispositioned and transferred to KSC for completion.

10.3 LEFT WING PROCESSING (STS-109)

Once Columbia was delivered to KSC in March 2001, the outstanding main landing gear work was completed. This work included the left inboard axle rework to improve brake clearance and the completion of the rotational pin inspections. The elevon flipper doors had a few PRs for Wear and tear issues that were resolved. The lower elevon cove columbium seals/springs were out of configuration as compared to drawing requirements, and minor adjustments were successfully made. When it was discovered that there was excessive corrosion protection coating applied to the elevon cove area,

work was done to clean that area. There was minor corrosion in the elevon cove area that was removed as well.

There were also numerous tile inspections and verifications performed during the processing flow for STS-109. No work was done on the wing leading edge RCC panels or Tee seals after Columbia returned from OMM and prior to STS-109. During that flow work was done on the LESS lower access panels 3, 6, 15, 17, 21, and 22 for step and gap issues and frayed horse collar gap concerns. Upper access panel 14 was replaced due to out-of-tolerance gap and out-of-tolerance Strain Isolation Pad (SIP). No lower tile acreage was replaced during the STS-109 flow, but the upper wing area had a few minor repair areas. All the leading edge and trailing edge panels for the left inboard elevon cove were replaced. Discrepancies were noted at Palmdale and corrected at KSC for the primary and secondary sealing circuits in the elevon cove seal assembly. The seals were operating within acceptable limits, but work was performed to repair leak paths and improve flow rate. There were 1,481 tiles that were suspect and had a manual deflection test performed on them in support of the corrective action required after one wing lower surface tile was found missing/debonded after the STS-103 (orbiter Discovery) mission. Thirteen thermal barriers were replaced in the main landing gear door area. There were 14 total MR items for STS-109.

10.4 LEFT WING PROCESSING (STS-107)

During the STS-107 flow, damage was noted to the left main landing gear axle sleeve and axle nut. A review of the entire shuttle fleet revealed similar conditions on other vehicles. The tire separation harness for the tire temperature and pressure measurements was found caught in the brake mechanism and had to be removed. The tires were deflated and removed in order to inspect the wheel half-tie bolts. Due to the discovery of corrosion in the tie bolt holes in wheels throughout the fleet, wheels with sleeved tie bolt holes were installed.

The angle seal at RCC panel 1 on the left wing leading edge (see Figure 10-4) was removed to support the evaluation of the horse collar gap filler between the adjacent tiles. During the removal attempt, the upper bushing remained bound with the shipside clevis. During subsequent attempts, the angle seal was manually manipulated to try and remove the preload. During the KSC paper review, structures engineers realized that the load applied to the angle seal was specified to be kept below 20 pounds, but was never recorded in the paper. The RCC specification requires that RCC panel loads be kept below 30 pounds. Subsequent tests at KSC verified that the angle seal load was below the 30-pound requirement. The LESS prevention and resolution team is addressing the issue of how to measure the load and how to support the seal in future operations. Work continued on the elevon flipper doors. Flipper door 1 blade seal was not making contact with the rub channel, potentially leading to excessive venting from the elevon cove area. This issue surfaced twice during this flow and was Material Review (MR) accepted to fly as is. Modification was made to the Inconel trailing edge seal and bulb seal on the elevon. Additional work was performed on the elevon cove corrosion protection again to reduce the excessiveness of the application.

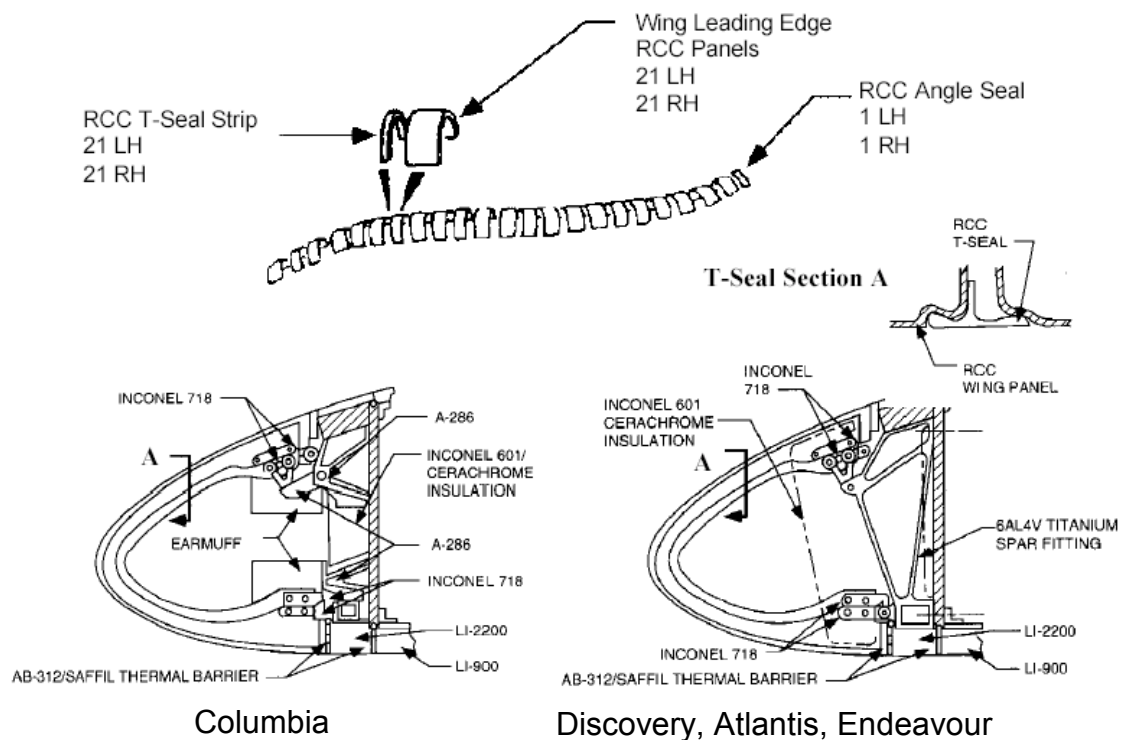


Figure 10-4. Wing leading edge RCC

An uncharacteristic number of access panels were removed during the STS-107 processing flow. Most of the upper (14 of 22) and lower (13 of 22) access panels were removed due to misinterpreted requirements to check for excessive movement in the panels. Wing leading edge upper and lower access panels at RCC 15 had to be removed to retrieve a burned ball of tape that had been inadvertently left from previous work performed during OMM. Upper access panel 18 was removed to investigate the possibility of water intrusion from a water deluge system mishap in the orbiter processing facility, but no damage was noted. Tee seal 10 was removed and shipped to the vendor for repair. No other wing leading edge RCC panels were removed in preparation for the STS-107 mission. Only one access panel was replaced on the left outboard elevon cove area, but there were three other minor tile repairs performed on the left elevons. There were four tiles replaced on the under side of the left wing in front of the left outboard elevon because a gap filler had protruded 0.8 inches. This caused charred filler bar, SIP damage, and instrumentation wiring damage. None of the tiles in these areas is believed to affect the failure scenario. There were 36 total MRs for STS-107.

10.5 RCC DESIGN

The RCC material is the basic structure of the wing leading edge panels (Figure 10-4), the nose cone, the chin panel between the nose cone and the nose landing gear door, and the forward external tank attach fitting cover plate on the orbiter. Its purpose is to protect the orbiter from local temperatures in excess of 2300 °F. Most RCC panels are designed with a 100-mission fatigue life, but RCC panels 8 through 12 have reduced lives due to higher temperature exposures. Panel 9 has the shortest mission life of 61 missions because it has the highest heating load during entry. RCC panel 17 has the highest aerodynamic load.

The panels were originally arc jet tested. Test data indicated that the multi-use temperature limit of 2960 deg F could be sustained for approximately 600 seconds. They were structurally tested up to a 1.2 factor of safety and eventually certified by analysis up to a 1.4 factor of safety. With these parameters, the panels are certified to 140% of their expected load up to the ultimate strength of the panel. Other significant testing of the RCC panels was not performed due to lack of sufficient time to accomplish the testing prior to the first flight of Columbia. RCC panels show no obvious aging effects due to calendar life, but the panels normally lose mission life due to the combined effects of oxygen, high temperature, and high pressure during the entry of each mission.

On Columbia, the structure supporting the RCC panels consisted of four attach fittings to mount each RCC panel to the aluminum honeycomb wing leading edge spar. In an effort to reduce the orbiter weight, wing components affecting the RCC installation were redesigned on subsequent vehicles. Beginning with the orbiter Discovery, the RCC attachment was accomplished using a single titanium attach fitting. The wing leading edge spar became a corrugated aluminum structure. Additional insulation was installed behind each RCC panel on all orbiters to shield the underlying structure from radiative heat damage from the high temperatures that the RCC reaches during entry.

The RCC is composed of a carbon-based substrate (see Figure 10-5) that provides essentially all of the RCC strength. It is composed of graphitized rayon fabric impregnated with a phenolic resin called Tetraethyl Orthosilicate (TEOS) to provide internal protection against porosity within the laminate. The substrate is covered with a silicon carbide coating also enhanced with TEOS and sealed with a sealant to protect it from oxidation within the substrate. The silicon carbide coating provides no thermal protection for the RCC.

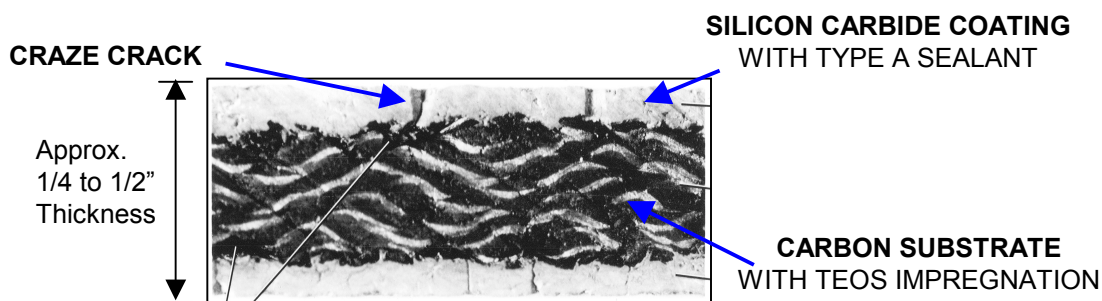


Figure 10-5. RCC cross section

During the manufacturing process, the silicon carbide surface acquires surface craze cracks due to differential contraction during the cooling process. The silicon carbide coating cools faster and contracts more than the carbon substrate during the cooling process. The craze cracks sometimes extend completely through the silicon carbide coating to the carbon substrate. A sodium silicate solution called “Type A Sealant” is applied to the silicon carbide coating to decrease porosity in the surface and fill the crazing cracks. Any erosion of the type A sealant and/or the silicon carbide coating could lead to direct exposure of the carbon fibers in the substrate. This provides a path for oxidation and can potentially lead to subsequent burn through of the RCC panel during entry. Development tests for the RCC never identified a susceptibility to oxidation; therefore, Columbia was not treated with the type A sealant until after the first five flights. Beginning in 1992, a double type A (DTA) sealant program was instituted on all vehicles to further enhance the corrosion protection on the wing RCC.

Each time a vehicle returns from space, the entire RCC and Thermal Protection System (TPS) are visually inspected to determine the extent of any damage. Inspections look for RCC impact damage and any indications of flow in the interface between the TPS (tiles) and adjacent RCC. There also exists a test method whereby the RCC panel is pressed with a gloved hand in the vicinity of RCC cracks to determine the integrity of the panel and the existence of potential unacceptable subsurface oxidation. This same test is always performed on RCC panels 6 through 17 near each of the adjoining Tee seals. During each OMM, all RCC components are visually inspected including all the attachment hardware and underlying attachment structure.

During the inspections, a determination is made to either repair, refurbish, or replace the panel as necessary. Repairs are required when there is noticeable damage to the surface of the panel. Field repairs can be made at KSC or Palmdale unless the carbon substrate is exposed. In that case the panels must be sent to the vendor for repair. Refurbishment is required at regular intervals to recoat the panels to increase their resistance to oxidation and mass loss. Occasionally, complete replacement of RCC panels is necessary due to unrepairable damage. Each wing leading edge RCC panel is paired with an associated Tee seal and both of these components are generally replaced/refurbished as a unit.

Columbia has only had three panels/Tee seals replaced over its history. Panels 12R and 10L were removed for destructive testing and pinhole evaluations. Panel 11L had fit problems and was sent to spares. Also, over Columbia's lifetime, seven RCC panels and six seals on the left wing were repaired, and 11 panels and 12 seals were refurbished. All of the Columbia RCC panels were within their predicted mission life limits, and most were original panels.

10.6 RCC IMPACT RESISTANCE

The RCC was not considered part of the TPS for the purposes of impact resistance. The TPS was designed to accommodate particle impacts, such as from hail, rain, runway debris, etc., whose impact energy did not exceed 0.006 foot-pounds to the surface. The wing leading edge RCC impact resistance allowed no damage to the RCC with the application of up to 16 inch-pounds of energy. Figure 10-6 shows RCC impact resistance ranging from 4 to 26 inch-pounds depending on the increasing thickness of the RCC element. Different tests including low velocity and hypervelocity tests have been conducted to determine the actual impact resistance of the RCC. Test projectile materials have included nylon, glass, aluminum, steel, lead, and ice and have taken shapes of spheres, bullets, and cylinders. The test results vary widely and appear to be significantly dependent on impact velocity, projectile type, and angle of incidence of impact. Because of the variability of the test results, no actual impact resistance could be defined.

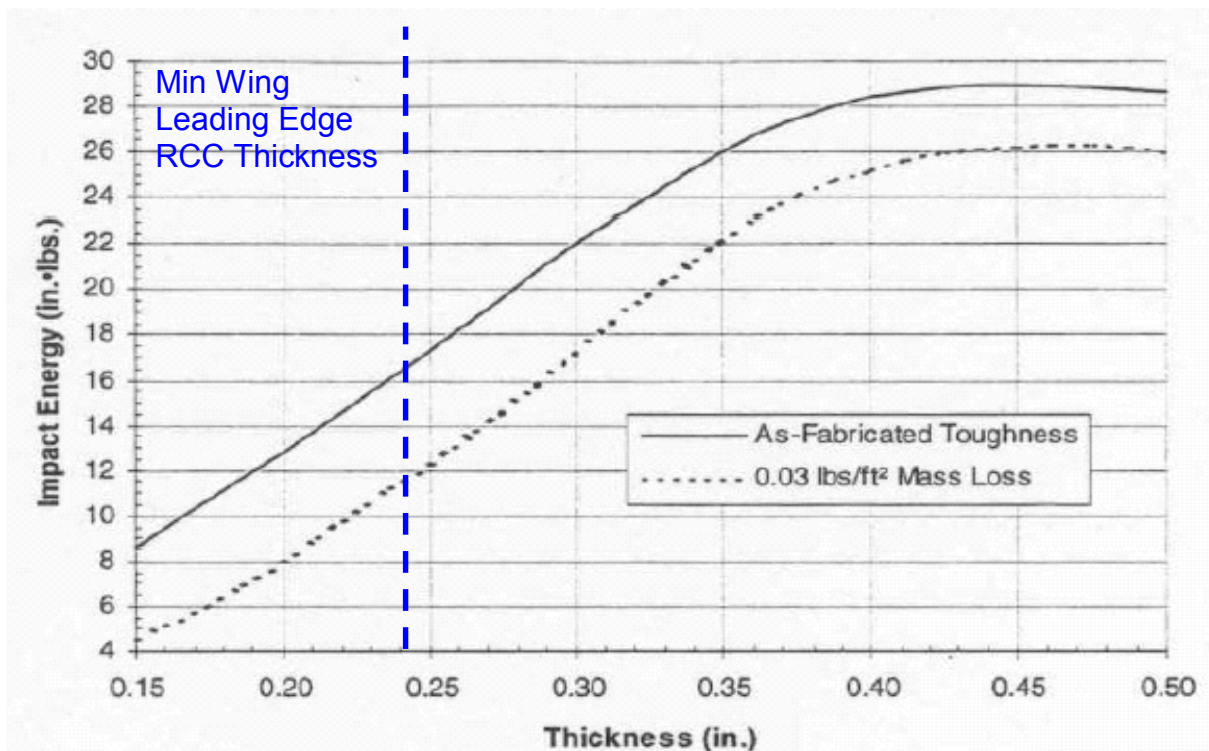


Figure 10-6. RCC impact resistance

In support of the STS-107 investigation, RCC impact testing was performed at Southwest Research Institute in San Antonio, Texas, by propelling a large piece of foam at high velocity at a previously flown RCC panel. These tests were described earlier in Section 3 and show that RCC material can be damaged by ET foam at impact velocities matching STS-107 debris impact conditions.

10.7 RCC CORROSION

The RCC panels are subject to mass loss due to loss of sealant that can be caused by normal entry heating, impact damage, or even undetected chemical attack. Mass loss results in a decrease in strength, burn resistance, and RCC mission life. Under the high temperatures of entry, the sealant may become molten in the vicinity of pinholes or debris impact areas and migrate, allowing an active oxidation process to begin at the surface. Some mass loss occurs normally during each mission. Mass loss is cumulative over mission life and is determined by analysis. Previously damaged RCC panels have been measured for mass loss using computer tomography, and that data is used in the analysis for all other RCC panels' mass loss determinations. When analysis shows that the 1.4 factor of safety can no longer be maintained, the RCC panel is removed from service. The silicon carbide sealant does not prevent mass loss, but it does help increase corrosion resistance. The sealant must be refurbished periodically, but is usually performed during the most convenient OMM that does not violate the limits listed in Table 10-1.

Table 10-1. RCC refurbishment limits

Panels	Refurbishment Interval
1-5, 20-22	As required based on visual inspection
6-17	16-18 missions, no calendar limit
18-19	32-36 missions, no calendar limit
Nose Cap	29 missions, no calendar limit

Subsurface oxidation has been discovered beneath the silicon carbide surface cracks in the sealant and coating which allow the oxidation process to thrive. This process is considered to be an impact to RCC mission design life, but is not generally considered to be a safety of flight issue. This oxidation process (Figure 10-7) starts with the breakdown of the coating due to entry heating. Surface craze cracks allow oxygen to migrate to the subsurface carbon fibers and react with them. This increase in oxidation develops into larger crazed areas, which eventually allow pieces to become dislodged due to vibration, aerodynamic, or thermal loads. Once the pieces dislodge, they leave a large path for the oxidation process to continue.

Dry ultrasonic and real-time radiographic inspections have been performed on the panels in the past to look at coating damage. More recently, special non-destructive

examinations are being evaluated which include infrared thermography to determine the extent of coating loss.

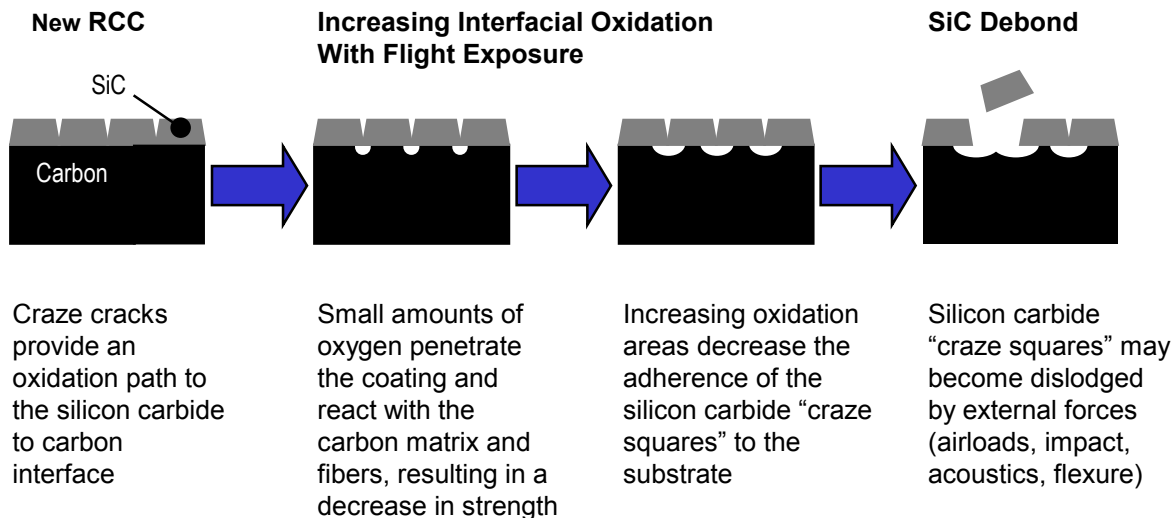


Figure 10-7. RCC corrosion process

Each wing leading edge RCC panel shares a Tee seal that is used to close the gap between adjacent RCC panels. Following STS-43 (Atlantis) in August 1991, routine inspections identified cracks in the web of a Tee seal. The cracks were in the silicon carbide coating and occasionally in the substrate, and were due to normal shrinkage. They were typically less than 1/2 inch long, were not visible to the naked eye, and usually occurred in the web of the seal, on the backside of the seal (Figure 10-8) near the apex rather than on the leading edge. Further examination of the remainder of the shuttle fleet identified 20 (of 132) cracked Tee seals. Columbia had 11 Tee seals identified with possible cracks. Detailed inspections determined that all the cracks were typical of the surface craze cracks in the coating. The Tee seal cracks were determined to be caused by warping of the substrate fabric during lay-up during the original build. The Tee seal cracking (Figure 10-9) leads to a reduction in mission life and loss of oxidation protection. All the seals were refurbished with new coating and sealant and were reinstalled. Failure analysis showed that cracks would form after excessive wishbone loading (bending) caused the brittle coating to crack. Crack testing was performed in 1991 on Tee seal 10 (attached to RCC panel 9) from the left wing of Columbia to try to determine the crack mechanism. The Tee seal was cycled 400 times in bending up to 70% of its ultimate load and no discernable damage was noted. After an engineering evaluation was performed on the health and strength of the Tee seal, it was subsequently reinstalled on Columbia.

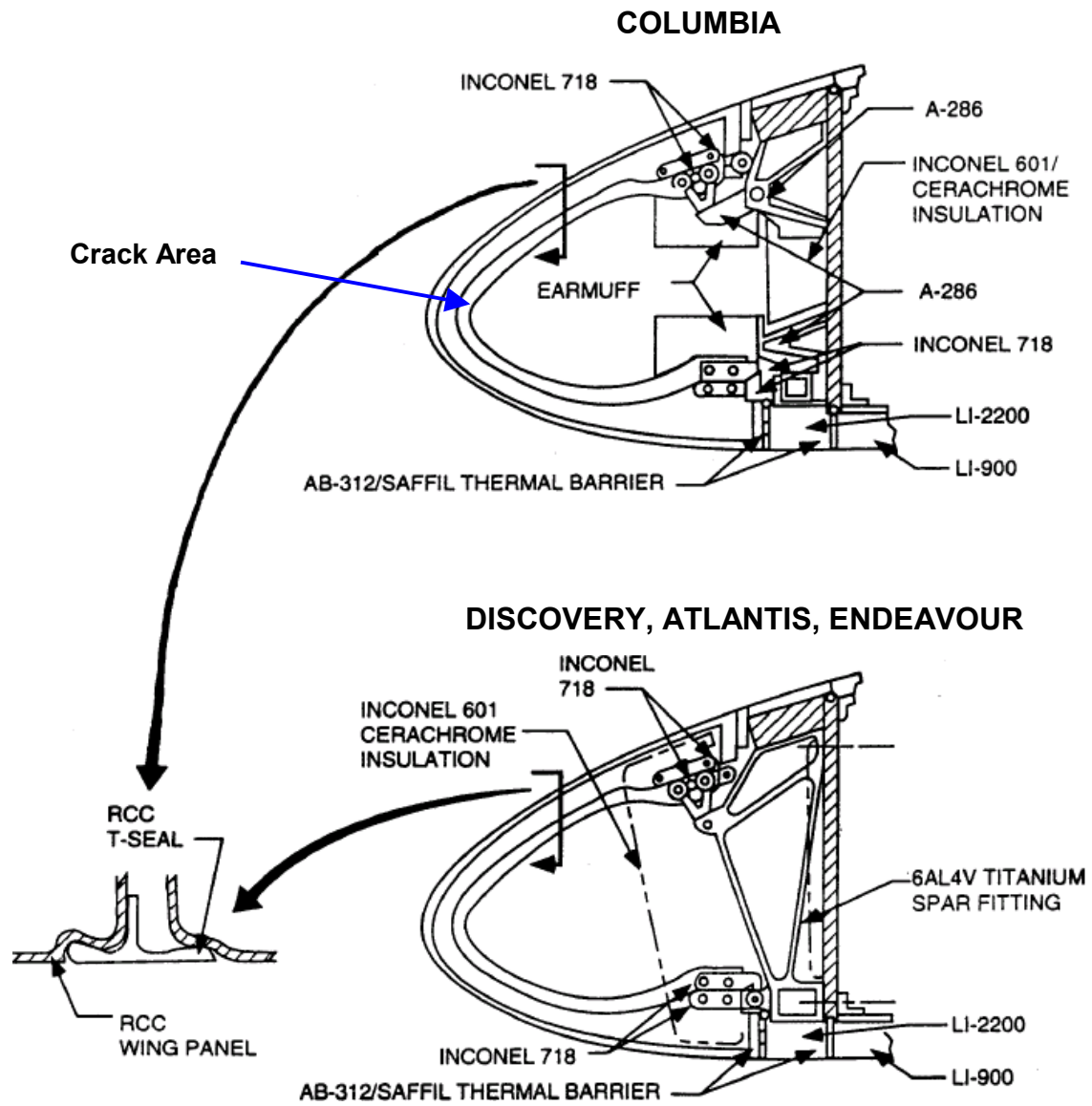


Figure 10-8. Tee seal crack location

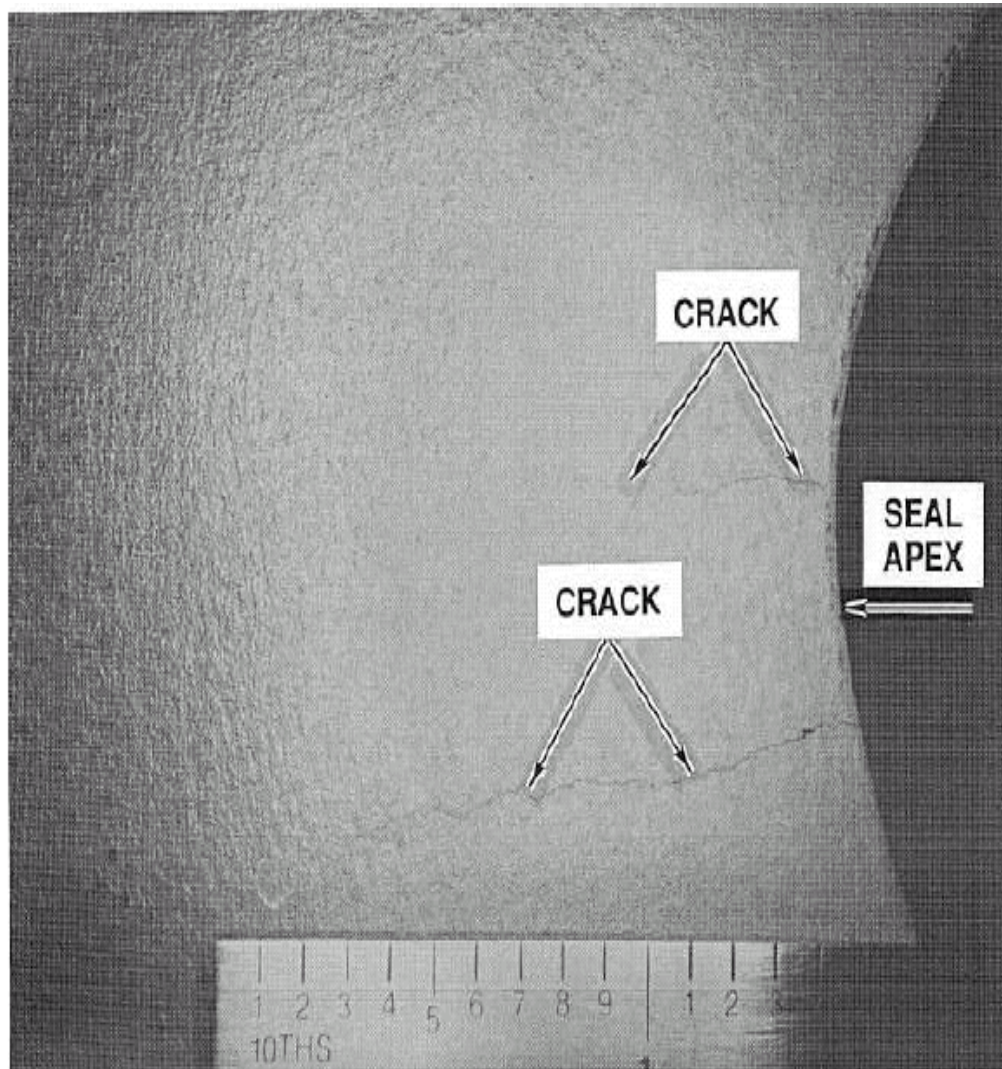


Figure 10-9. Tee seal cracking

Another phenomenon, discovered first on Columbia after STS-50 landed, was the existence of pinholes (Figure 10-10) in the RCC panels. The pinholes were found primarily in the wing leading edge RCC and were subsequently identified on all orbiters. Testing has shown that the pinholes are most likely the result of the accelerated oxidation process involving zinc oxide and the silicon carbide coating. The reaction of the zinc oxide and the silicon carbide produces a silica (glass) exudate that flows out of the pinhole area. The presence of zinc oxide is theorized to originate from the paint primer used to recondition the launch pad after each mission and is considered an accelerator to the oxidation process. The zinc-based contamination accumulates on the wing leading edge RCC as rainwater drips off of the launch pad. This contamination rests on the RCC without reacting to the surface material while at ambient conditions at the pad. All of the damaging oxidation occurs once the RCC is exposed to the high temperatures, pressures, and excess oxygen of re-entry. Only a few pinholes have been observed on the nose cap RCC, most likely because the nose

cap remains under a protective cover while at the launch pad. It is also believed that sodium chloride contributes to the oxidation process, but to a much lesser extent than the zinc oxide.

In 1997, pinhole acceptance criteria were established. Pinholes with surface dimensions less than 0.040 inches discovered during routine processing flows are acceptable to fly as is for up to 16 missions unless the carbon substrate is exposed, in which case the panel must be repaired. Pinholes discovered at OMM greater than 0.040 inches are unacceptable. Although the pinholes themselves constitute only a small mass loss, they are not considered to be a safety-of-flight issue by themselves. Analysis has identified that the sustainable thru-hole size in-flight due to orbital debris is 0.25 inches in the lower surfaces of RCC panels 5-13. A hole under 1 inch in diameter anywhere else in the RCC is considered survivable for a single mission.

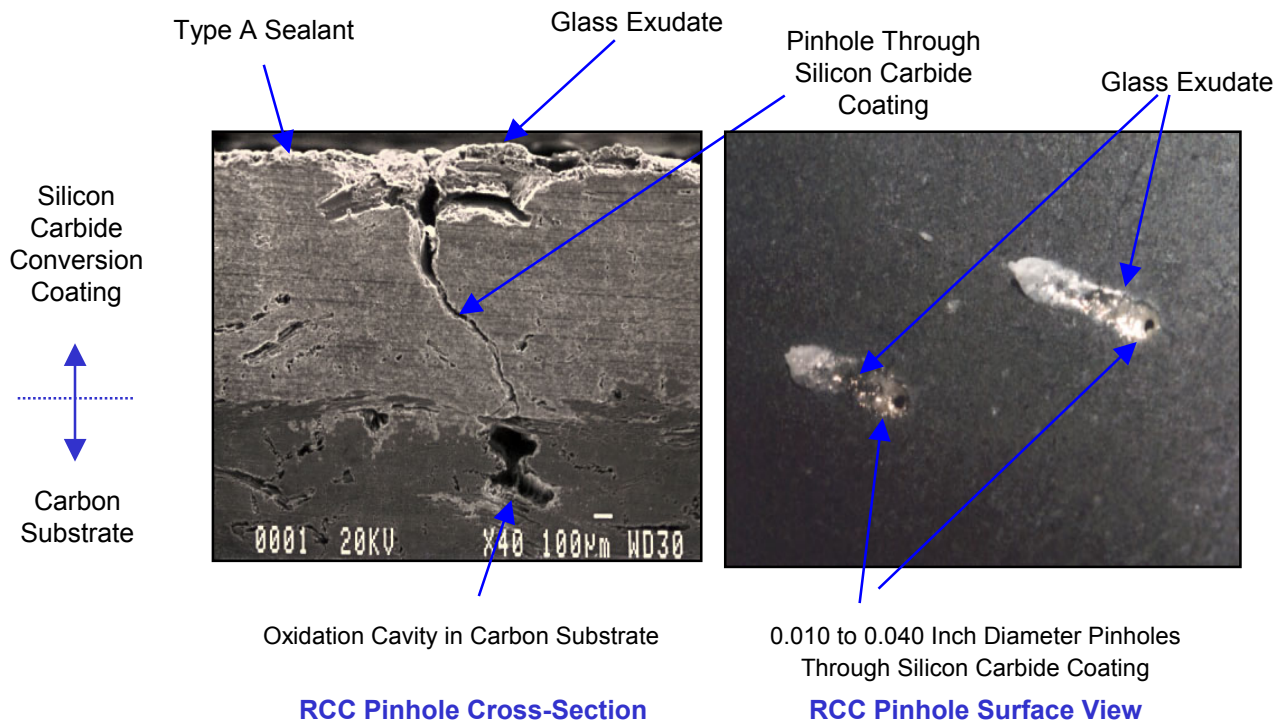


Figure 10-10. RCC pinholes

There have been damaged RCC panels that were discovered after the vehicle returned from space on various missions. Some of the impact damage was only to the surface, but some even caused damage to the coating on the backside of the panel. In 1992, after STS-45, significant impact damage (overall length of ~1.75 inches) was noted on RCC panel 10R on Atlantis. The damage (Figure 10-11) was theorized to come from Orbital debris or micrometeorite impacts during the mission. This type of RCC damage is of particular concern in that a significant impact could cause a hole in the RCC large enough to lead to wing spar burn through and subsequent loss of crew and vehicle. At that time, the maximum acceptable hole size (0.040”) criterion was established for

processing flows and advanced wing leading edge internal insulation was modified to reduce the risk should hot gas penetrate the RCC.

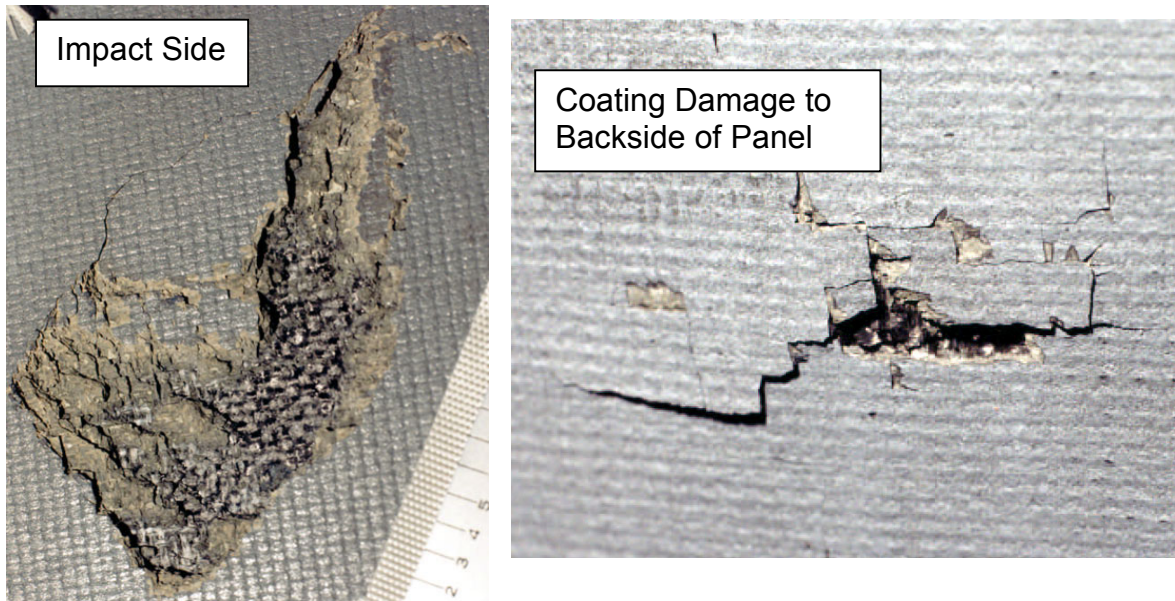


Figure 10-11. RCC impact damage

There has been a history of loose bolts on access panels on all orbiters. Following STS-87, the right-hand lower access panel 4 had a loose bolt. All other installations were inspected and several additional bolts were found with low torque. All bolts were subsequently torqued to their proper values. During STS-95, the OMS pod Y-web door area had some damaged insulation. It was determined post-flight that there were bolts in the area that had low torque. A review of other orbiters identified low torque bolts on Discovery and Endeavour. Low torque bolts were also found during Columbia's last OMM. The low torque was attributed to the performance of an improper torque sequence. All attach fittings were removed and reinstalled using the correct torque sequence.

11.0 EXTERNAL TANK

11.1 INTRODUCTION

The External Tank (ET) used for STS-107 was Light Weight Tank (LWT) number ET-93. This tank was the first LWT to be used with a cluster of three Block-II Space Shuttle Main Engines (SSMEs). As discussed in Section 3, there is significant visual and debris trajectory data to implicate the left bipod ramp area as the source of debris. Contributors to forward bipod thermal protection system (TPS) foam loss were: (1) the design, verification, and process validation did not encompass all material and processing variability or adequately address all failure modes, and (2) the acceptance testing and inspection techniques and procedures were not designed to be capable of rejecting ramps with adverse "as-built" features which would threaten the TPS integrity.

11.2 TPS REQUIREMENTS

During prelaunch, the ET TPS minimizes ice formation and maintains the quality of cryogenic propellant. During ascent, the ET TPS maintains the structure within design temperature limits. Program requirements (NSTS 07700, Vol. X, Book I, Paragraph 3.2.1.2.14) indicate that the ET "shall be designed to preclude the shedding of ice and/or other debris that would jeopardize the flight crew, vehicle, mission success, or would adversely impact turnaround operations." During ET entry, the TPS assures a predictable, low altitude ET break-up that meets the ET entry impact footprint boundary limits.

The ET TPS itself is designed to have low density to maximize Shuttle payload capacity, high adhesion to cryogenic surfaces (-423 °F), resistance to thermal abrasion and degradation from aerodynamic shear, consistency (material qualified is the material flying), and environmental resistance to ultraviolet radiation, rain, etc. The application of ET TPS materials includes computer controlled automatic spray cells and manual application in normal working environments.

11.3 HISTORY OF FOAM CHANGES AND DEBRIS EVENTS

The ET TPS history is marked by multiple material and configuration changes resulting from ET TPS and ice loss events, design enhancements, environmental regulations (especially blowing agent changes), and supplier changes. The history of foam changes is outlined in Figure 11-1, and Table 11-1 lists the ET flight history, as well as age and exposure data. Thousands of tests have been conducted to develop and qualify the ET TPS. There were no first time ET TPS changes on STS-107/ET-93 except for rework of the TPS on the upper aft ET/Solid Rocket Booster (SRB) fitting fairing (following SRB demate) using BX-265. Basic bipod TPS materials had not changed from the beginning of the program until after ET-93. The bipod TPS configuration has been stable since 1983, when with ET-14 the ramp angle was changed. At ET-76 in 1995, there was one minor change to the ramp intersection with the ET intertank area. At ET-116 in 2002, the bipod material was changed to BX-265, but ET-93 had been constructed with BX-250. No indication has been found that any specific ET TPS foam change or any combination of historical ET TPS foam changes alone caused the bipod foam loss on STS-107/ET-93.

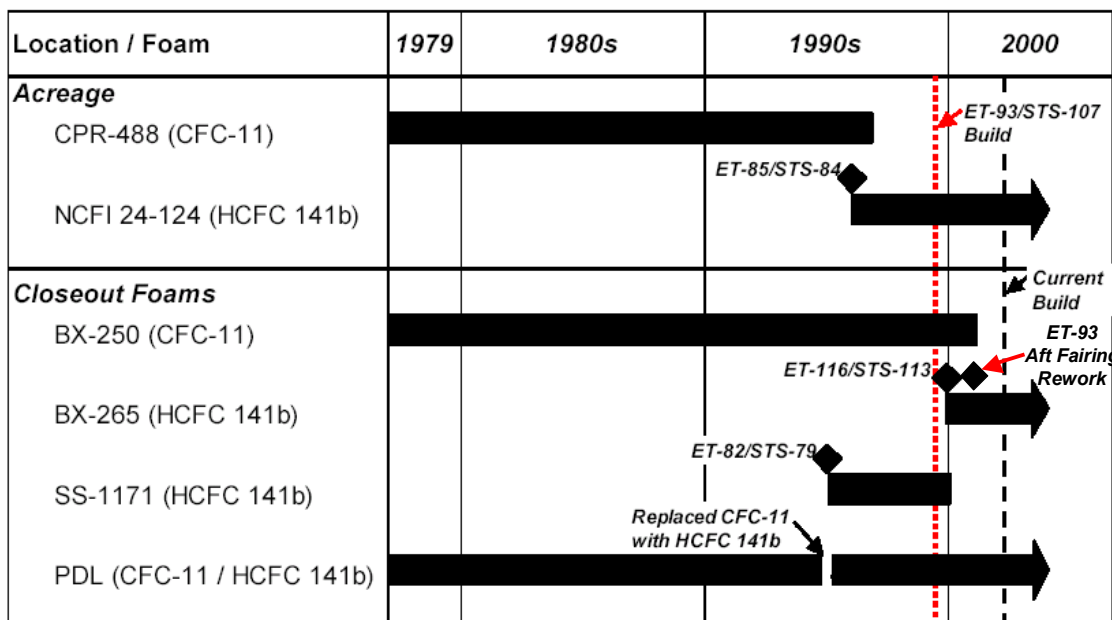


Figure 11-1. History of foam changes. Blowing agent shown in parentheses, no changes to SLA

Table 11-1. STS-Orbiter-ET configuration, age, and exposure

STS	STS aka	OV	ET	ET wt.	Date	ET Age @ Launch (days)	ET Exposure @ Launch (days)
1		Columbia	1	ET	04/12/81	653	105
2		Columbia	2	ET	11/12/81	258	74
3		Columbia	3	ET	03/22/82	175	35
4		Columbia	4	ET	06/27/82	161	33
5		Columbia	5	ET	11/11/82	169	52
6		Challenger	8	LWT	04/04/83	208	126
7		Challenger	6	ET	06/18/83	327	24
8		Challenger	9	LWT	08/30/83	230	29
9		Columbia	11	LWT	11/28/83	206	43
11	41B	Challenger	10	LWT	02/03/84	339	23
13	41C	Challenger	12	LWT	04/06/84	259	19
14	41D	Discovery	13	LWT	08/30/84	352	79
17	41G	Challenger	15	LWT	10/05/84	295	23
19	51A	Discovery	16	LWT	11/08/84	286	17
20	51C	Discovery	14	LWT	01/24/85	448	20
23	51D	Discovery	18	LWT	04/12/85	353	16
24	51B	Challenger	17	LWT	04/29/85	409	33
25	51G	Discovery	20	LWT	06/17/85	347	14
26	51F	Challenger	19	LWT	07/29/85	431	31
27	51I	Discovery	21	LWT	08/27/85	398	22
28	51J	Atlantis	25	LWT	10/03/85	287	35
30	61A	Challenger	24	LWT	10/30/85	348	15
31	61B	Atlantis	22	LWT	11/26/85	459	15
32	61C	Columbia	30	LWT	01/12/86	208	42
33	51L	Challenger	26	LWT	01/28/86	319	38
26R		Discovery	28	LWT	09/28/88	1261	87
27R		Atlantis	23	LWT	01/02/89	1561	62
29R		Discovery	36	LWT	03/13/89	1189	39
30R		Atlantis	29	LWT	05/04/89	1450	44
28R		Columbia	31	LWT	08/08/89	1484	25
34		Atlantis	27	LWT	10/18/89	1723	51
33R		Discovery	38	LWT	11/22/89	1317	27
32R		Columbia	32	LWT	01/09/90	1609	43
36		Atlantis	33	LWT	02/28/90	1597	35
31R		Discovery	34	LWT	04/24/90	1674	40
41		Discovery	39	LWT	10/06/90	1635	32
38		Atlantis	40	LWT	11/15/90	1609	88
35		Columbia	35	LWT	12/02/90	1850	164
37		Atlantis	37	LWT	04/05/91	1906	22
39		Discovery	46	LWT	04/28/91	1327	49
40		Columbia	41	LWT	06/05/91	1776	35
43		Atlantis	47	LWT	08/02/91	1323	39

**Table 11-1. STS-Orbiter-ET configuration, age, and exposure
(continued)**

STS	STS aka	OV	ET	ET wt.	Date	ET Age @ Launch (days)	ET Exposure @ Launch (days)
48		Discovery	42	LWT	09/12/91	1829	32
44		Atlantis	53	LWT	11/24/91	846	33
42		Discovery	52	LWT	01/22/92	994	35
45		Atlantis	44	LWT	03/24/92	1840	34
49		Endeavour	43	LWT	05/07/92	2005	56
50		Columbia	50	LWT	06/25/92	1333	23
46		Atlantis	48	LWT	07/31/92	1561	51
47		Endeavour	45	LWT	09/12/92	1923	19
52		Columbia	55	LWT	10/22/92	994	27
53		Discovery	49	LWT	12/02/92	1577	25
54		Endeavour	51	LWT	01/13/93	1440	42
56		Discovery	54	LWT	04/08/93	1256	25
55		Columbia	56	LWT	04/26/93	1082	79
57		Endeavour	58	LWT	06/21/93	979	55
51		Discovery	59	LWT	09/12/93	900	80
58		Columbia	57	LWT	10/18/93	1180	33
61		Endeavour	60	LWT	12/02/93	889	36
60		Discovery	61	LWT	02/03/94	842	25
62		Columbia	62	LWT	03/04/94	773	23
59		Endeavour	63	LWT	04/09/94	737	22
65		Columbia	64	LWT	07/08/94	718	24
64		Discovery	66	LWT	09/09/94	591	23
68		Endeavour	65	LWT	09/30/94	697	47
66		Atlantis	67	LWT	11/03/94	535	25
63		Discovery	68	LWT	02/03/95	546	25
67		Endeavour	69	LWT	03/02/95	484	23
71		Atlantis	70	LWT	06/27/95	495	63
70		Discovery	71	LWT	07/13/95	435	58
69		Endeavour	72	LWT	09/07/95	433	59
73		Discovery	73	LWT	10/20/95	381	54
74		Atlantis	74	LWT	11/12/95	360	33
72		Endeavour	75	LWT	01/11/96	342	37
75		Columbia	76	LWT	02/22/96	330	25
76		Atlantis	77	LWT	03/22/96	303	24
77		Endeavour	78	LWT	05/19/96	307	34
78		Columbia	79	LWT	06/20/96	281	23
79		Atlantis	82	LWT	09/16/96	188	38
80		Columbia	80	LWT	11/19/96	368	35
81		Atlantis	83	LWT	01/12/97	262	34
82		Discovery	81	LWT	02/11/97	390	26
83		Columbia	84	LWT	04/04/97	291	25
84		Atlantis	85	LWT	05/15/97	281	22
94		Columbia	86	LWT	07/01/97	266	21
85		Discovery	87	LWT	08/07/97	246	25

Table 11-1. STS-Orbiter-ET configuration, age, and exposure (concluded)

STS	STS aka	OV	ET	ET wt.	Date	ET Age @ Launch (days)	ET Exposure @ Launch (days)
86		Atlantis	88	LWT	09/25/97	251	39
87		Columbia	89	LWT	11/19/97	146	22
89		Endeavour	90	LWT	01/22/98	167	35
90		Discovery	91	LWT	04/17/98	154	26
91		Discovery	96	SLWT	06/02/98	141	32
95		Discovery	98	SLWT	10/29/98	147	39
88		Endeavour	97	SLWT	12/04/98	249	47
96		Discovery	100	SLWT	05/27/99	183	24
93		Columbia	99	SLWT	07/23/99	360	47
103		Discovery	101	SLWT	12/19/99	24	37
99		Endeavour	92	LWT	02/11/00	298	61
101		Atlantis	102	SLWT	05/19/00	473	56
106		Atlantis	103	SLWT	09/08/00	444	26
92		Discovery	104	SLWT	10/11/00	498	31
97		Endeavour	105	SLWT	11/30/00	503	31
98		Atlantis	106	SLWT	02/07/01	418	30
102		Discovery	107	SLWT	03/08/01	455	25
100		Endeavour	108	SLWT	04/19/01	434	29
104		Atlantis	109	SLWT	07/12/01	435	22
105		Discovery	110	SLWT	08/10/01	380	40
108		Endeavour	111	SLWT	12/05/01	258	36
109		Atlantis	112	SLWT	03/01/02	358	38
110		Atlantis	114	SLWT	04/08/02	294	28
111		Endeavour	113	SLWT	06/05/02	401	38
112		Atlantis	115	SLWT	10/07/02	376	28
113		Endeavour	116	SLWT	11/23/02	360	43
107		Columbia	93	LWT	01/16/03	805	39

ET debris has been observed throughout program history, including both ET TPS and ice debris. Since STS-1, imagery was available on about 80 missions, and debris has been confirmed on at least 62 missions. At least six missions lost portions of the left bipod ramp (see Section 3.5). TPS loss on the right bipod ramp has never been observed. A portion of the left bipod ramp was lost during STS-112 ascent and impacted the left SRB Integrated Electronics Assembly. No changes were made to STS-113 or STS-107 bipod ramp configurations after this event.

The majority of ET debris events have been limited to small mass (< 0.2 lbs). A definitive correlation to orbiter damage is difficult except for major debris events such as STS-27R, which was identified as SRB ablator debris, and STS-87, which was attributed to ET intertank foam loss. Based on available historical data, the bipod ramp represents the source of the largest pieces of ET debris (estimated > 1.0 lbs), and LO2 feedline bellows ice is second (estimated < 0.3 lbs).

11.4 STS-107/ET-93 CHRONOLOGY

Ascent film indicates that the origin of STS-107 ET TPS loss was from the forward bipod area (see Section 3). Image-based size estimates support this to be the bipod ramp rather than flange or acreage foam. The history of bipod TPS loss provides additional supporting evidence. Available data supports the bipod ramp as the most probable point of origin of STS-107 debris.

11.4.1 Bipod Ramp TPS Configuration

The forward bipod TPS configuration includes a complex combination of foams, Super Light Ablator (SLA), and underlying bipod structural substrate elements. The bipod ramp configuration has been essentially stable since early in the program. There have been no changes in material until after ET-93 and only minimal changes to configuration, processing, and personnel certification and training. The BX-250 ramp angle has been constant since 1983, when with ET-14, the ramp angle was changed to 30° maximum with a 5.0 ±1.0 inch radius at the forward edge (changed from 45° ± 5.0° with no radius at the forward edge). This was changed as a result of suspected foam debris on STS-7/ET-6. For ET-76 in 1995, there was one minor change to the forward ramp intersection with the ET intertank area; the 5.0 ±1 inch radius was changed to a straight termination line with a 0.25-inch step allowed. At ET-116 in 2002, the bipod material was changed to BX-265, but ET-93 was BX-250. There has been no indication that the bipod ramp configuration changes affected the observed STS-107/ET-93 bipod foam loss.

11.4.1.1 Left and Right Bipod Ramp Differences

TPS loss on the right bipod ramp has never been observed. Launch/ascent imagery from ground assets is less favorable for seeing right bipod foam loss as compared to the left bipod, and post-ET separation crew imagery is random between imaging the left or right bipod ramps.

There is no flight or test data to explain why the -Y (left) bipod loses foam and the +Y (right) does not. The Shuttle Program only provides the -Y ramp air loads as a worst case for ET project analysis. There are several bipod configuration differences that may contribute to foam not coming off the +Y ramp. First, the foam ramp is configured slightly differently to accommodate the inboard strut for the LO2 feed line support structure (see Figure 11-2). Second, the proximity of the right bipod to the LO2 feedline could potentially influence local surface pressure causing a lower internal to external pressure differential (see Figure 11-3). Finally, the outboard and aft facing surface of the -Y bipod may experience lower surface pressure due to flow separation and other local effects relative to the +Y side. If the internal ramp pressure was high due to adverse “as-built” features in the ramp, this could lead to a higher differential pressure on the -Y versus the +Y ramp. However, the aerodynamic loads analysis reviewed in Section 3.5 shows that the loads on both ramps are below their design requirements.

+Y Bipod with ramp complete showing feed line and location of foam cut out to accommodate strut

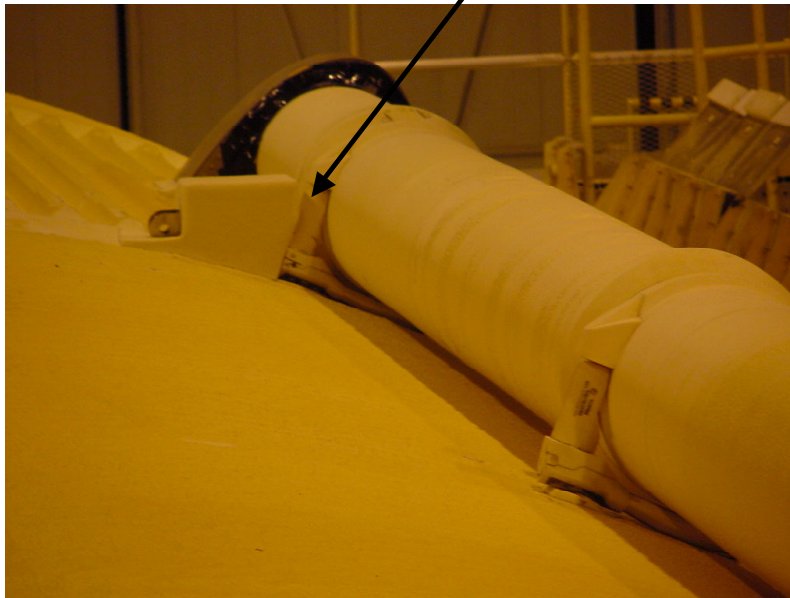
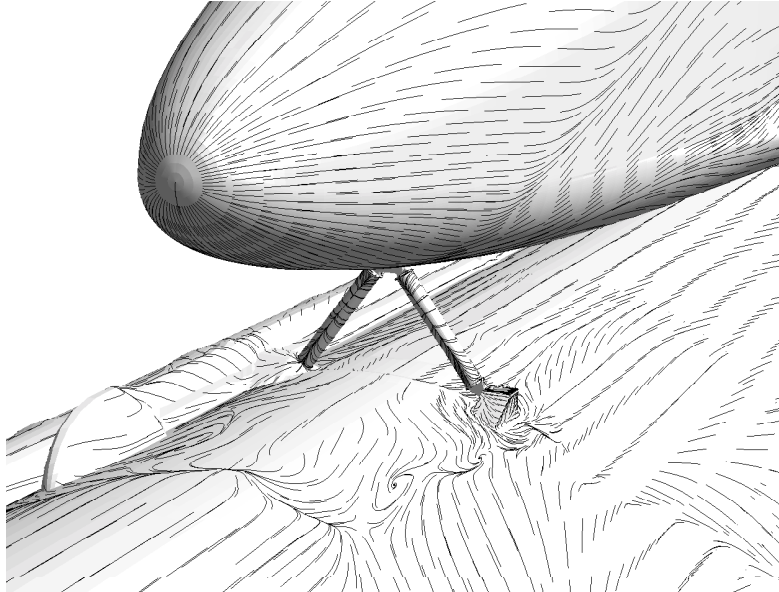


Figure 11-2. Right (+Y) bipod ramp



JSC CFD Results: Mach No. = 2.46, Alpha = 2.08°

Figure 11-3. Left and right bipod ramp flow differences, CFD results

11.4.2 Bipod Ramp Certification

The BX-250 foam was supplied to the ET project as a flight verified material from the Saturn Program. A review of material properties certification indicated forward bipod materials met material performance requirements including thermal recession properties at design ascent heating rates, thermal conductivity to preclude ice formation and to maintain cryogenic propellant quality during prelaunch, and mechanical properties.

Process validation was performed by similarity of “flight-like” design substrate configurations. There had been no specific bipod dissection prior to the STS-107/ET-93 investigation. Dissection of the bipod ramps from the production flow provided insight that the bipod ramp could contain unique adverse “as-built” features. The features identified during these recent dissections could potentially reduce the strength of the foam and result in foam failure and subsequent debris.

For the bipod ramp, there was no robust evaluation of the manual spray process. The complexity of the manual spray process of the forward bipod TPS closeout leads to unique defects in this area including voids, rollovers, and TPS discontinuities. The configuration of the forward bipod BX-250 foam was verified based on similarity to the Protuberance Air Load (PAL) ramp, which did not address all aspects and failure mechanisms in combination with critical environments (adverse “as-built” features). The interaction of the underlying SLA configuration interfacial boundary and the potential effects of cryopumping were not considered. The design, verification, and process validation did not encompass all material and processing variability or adequately address all failure modes.

11.4.3 Bipod Ramp Build Process

Experienced certified practitioners performed the ET-93 bipod ramp BX-250 sprays, each with over 20 years experience. No indications of sprayer error were found. Procedures were followed and documented, and processes were within control limits (e.g., material specifications, temperature, and humidity) except that the process plan review found no Quality Control (QC) verification of overlap timing. There is no requirement to verify the overlap timing, and the impact of the overlap timing verification is not known.

Dissection results of five ET TPS configurations demonstrated the forward bipod as the configuration with the most significant defects. Defects are driven by the variable manual spray process and complex contour substrate. This creates the potential for a combination of large voids or defects at critical locations needed to produce a significant foam loss. The designed-in process plan controls related to QC buy-off of critical parameters did not preclude introduction of adverse “as-built” features resulting from the complex and variable forward bipod manual spray operation. There is also variability in the response of the foam based on inherent randomness of the foam cell structure. It may not be possible to control a manual process well enough to preclude defects in the bipod ramp.

11.4.4 Bipod Ramp Foam Acceptance/Non-Destructive Evaluation

ET BX-250 ramp foam build acceptance processes include localized plug pull and core tests of the ramp material prior to final trim configuration. The plug-pulls are taken from trimmed-off over-spray lead-in/lead-out areas (witness, or sample panels) on either side of the ramp to provide density, final visual inspections, and dimensional features. Post-build inspection techniques are limited to visual inspections only. There were no anomalies found with the STS-107/ET-93 forward bipod ramp using inspection and acceptance techniques available at Michoud Assembly Facility (MAF).

Previous efforts to implement robust foam Non-Destructive Evaluation (NDE) techniques were unsuccessful (a variety of techniques were attempted). Some progress was made in certain areas, but it never reached a fully qualified approach and the MAF effort was discontinued in 1993. Development efforts found many false positives and many missed defects. NDE methods in use at MAF were not able to identify adverse “as-built” features in the forward bipod BX-250 ramp, which could combine with nominal environments and create debris. Acceptance testing and inspection techniques and procedures were not designed to be capable of rejecting ramps with adverse “as-built” features that would threaten the TPS integrity.

11.4.5 ET Shipping and Handling

Post-build activities include storage at MAF, shipment to Kennedy Space Center (KSC), storage at KSC, and mating to the SRBs and orbiter. Extensive documentation governs the steps taken to care for the ET. Documentation review found no issues in ET-93 processing paperwork. Storage took place in locked, limited-access facilities. The tanks were shipped pressurized with nitrogen to 6.0 ± 0.5 psi per requirements. At KSC, the LH2 tank pressurant is changed to helium and the pressure on each tank is checked at least twice per week per requirements. Visual inspections were performed every 90 days while in storage. ET-93 was inspected seven times between arrival at KSC and launch, not counting additional daily inspections when mated to the SRBs. Processes were in place and followed to ensure that shipping and handling were performed in a manner that minimizes damage to the ET.

11.4.6 KSC Processing Activities

The shuttle flight manifest was delayed due to cracks found during inspections of Main Propulsion System feedline flow liners on Atlantis in June 2002. The final manifest moved STS-112 and STS-113 ahead of STS-107. ET-93 was de-mated from SRBs BI-114/RSRM-86 and later mated to SRBs BI-116/RSRM-88, and SRBs BI-114/RSRM-86 were used for STS-113. All mate/de-mate operations were carried out in accordance with standard procedures, and are outlined in Figure 11-4. There are no indications that KSC ET processing (ET shipping, handling, and processing) contributed to the bipod foam loss on STS-107/ET-93.

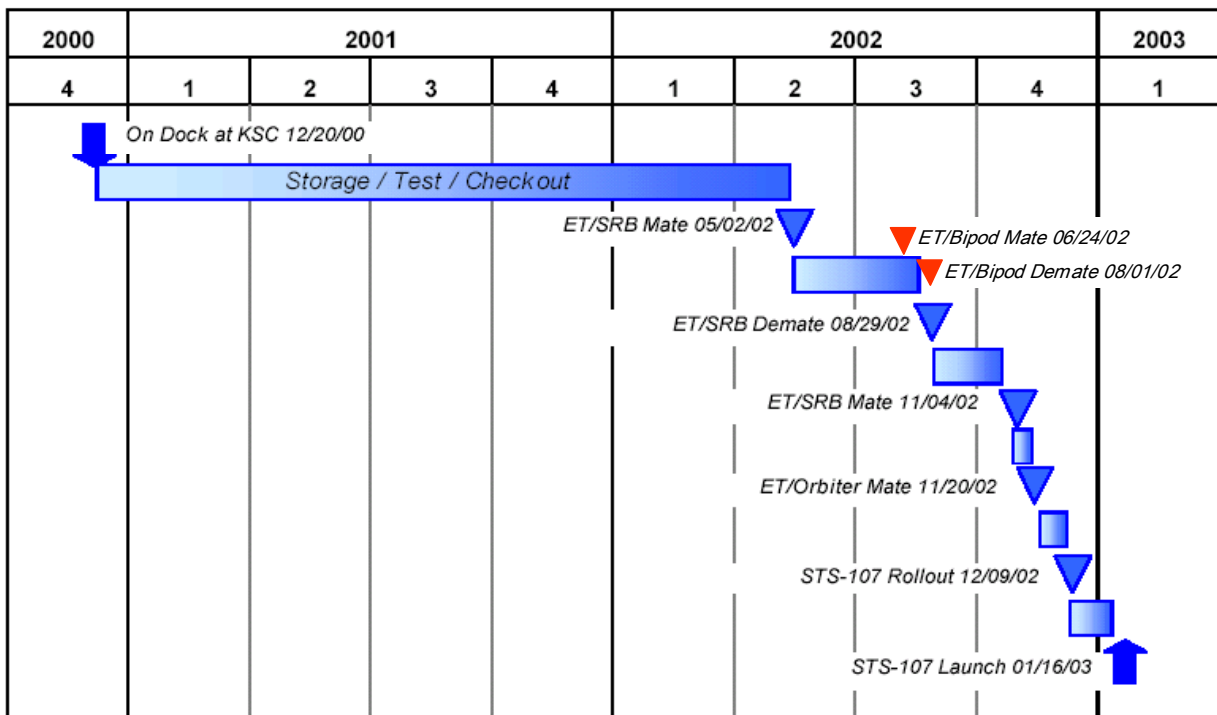


Figure 11-4. ET-93 processing timeline at KSC

11.4.6.1 ET-93 Mate/De-Mate/Re-Mate

The ET-93 bipod struts were installed, and then later removed during de-mate and re-installed. This process has been performed at least six times during the Shuttle program. ET-11 was used on STS-9, but there is no imagery to confirm ET foam loss. ET-13 was used on STS-14 (41D), but again there is no imagery to confirm ET foam loss. ET-23 was used on STS-27R with handheld video imagery available that does not show the bipod ramps, but no foam loss was observed elsewhere. ET-23 was mated and de-mated during checkout of the Vandenberg Air Force Base facilities. STS-27R had a great amount of tile damage thought to be due to the loss of SRB ablator during launch. ET-37 was used on STS-38 but there is no imagery to confirm ET foam loss. ET-80 was used on STS-80, and there were two lost divots on the flange under the bipod and one 10-inch diameter divot on the intertank forward of the bipods. ET-86 was used on STS-94 and the left bipod strut was installed upside down then re-installed correctly. The bipod ramps were visible and no bipod foam loss was noted.

11.4.6.2 ET-93 Crushed Foam

On ET-93, crushed foam (1.5" x 1.25" x 0.187") was seen after the -Y strut removal at the clevis. The thickness of foam in this area is 2.187 inches. Exposed crushed foam is not permissible outside of specific acceptance criteria, so a Problem Report (PR VG-389216) was written to evaluate the condition. The crushed foam was essentially covered up after mating to a new set of bipod struts. No data is available to determine

if this section of foam could have been the source of, or contributed to, a void or leak path for liquid or gas.

Inspection of the region after installation of the bipod struts showed that the crushed foam did not extend farther than 0.75" beyond the bipod fitting-clevis joint, which is within acceptable limits. Dye penetration testing with recreated conditions indicated that the damage extended 0.25 inches from the visible mark and 0.5 inches into the surface of the foam, where the damage stopped.

The Material Review Board (MRB) decided to "use as is," and STS-107 launched with crushed foam contained behind the -Y bipod strut clevis. Crushed foam in this area is a nominal configuration, and the PR was only written for documentation for bipod strut removal and future inspections. Available data indicates that every flight may have crushed foam beneath the bipod strut. Review of the ET-93 PR, MAF testing, and the ET-117 strut removal provided evidence that crushed foam had no impact on performance, both thermal and structural. Data are inconclusive as to whether the crushed foam and bipod foam loss are associated.

11.4.7 ET Pre-launch Operations

The electrical system performance was nominal based on evaluation of pre-launch data and post flight inspection of ground electrical interfaces and SRB hardware. No anomalous conditions were identified during STS-107 visual inspections during launch operations: preflight, tanking ice team, video surveillance, and postflight walk down. There are no indications that ET pre-launch operations at KSC contributed to bipod foam loss on STS-107/ET-93.

11.4.8 Launch/Ascent

The ET-93 propulsion system performance was within design limits based on preflight predictions and postflight reconstruction. Comparison to historical performance showed performance within flight history experience for LWT, Super Light Weight Tank (SLWT), and Block II SSME. The STS-107 trajectory was within design limits throughout ascent. There were no anomalous angles of attack or dynamic pressure indications (see Section 3.5). STS-107 reconstructed air loads were within design limits, and no unique observations were associated with STS-107/ET-93. It is unlikely that any significant bipod structural loads were associated with the 62 second wind shear event followed by a 0.6 Hz RSRM gimbal reaction associated with LO2 slosh (see Section 3.5 and sections below). No anomalous structural loads have been identified. Best-estimated trajectory loads and flex body loads assessment reconstructions show the ET interfaces to be well within design limits. Bipod interface vehicle loads are not considered "driving" environments for the bipod foam ramp. Adjacent structural stiffness precludes significant induced bipod ramp deflections from the interface strut loads. The majority of flexural loading on the bipod ramp results from cryogenic shrinkage of the LH2 tank prior to lift-off. STS-107 ascent thermal environments were within design limits based on analysis of flight data and ET system performance. A higher LH2 tank ullage preflight pressurization pressure (pre-press) is required for flights with Block-II SSME clusters. This helps

reduce spikes in the high-pressure fuel turbopump turbine discharge temperatures during start. The LWT was certified for higher pre-press and approved for ET-92 and subsequent flights by Interface Revision Notice (IRN) IC-1432 on 8-28-98.

Data are inconclusive as to whether the STS-107 ascent environments contributed to the bipod foam loss on ET-93.

11.4.8.1 ET LO2 Slosh Baffle Changes

Eight ET LO2 slosh baffles were used until ET-14 in 1983. Vehicle stability analysis based on development flight instrumentation confirmed minimum LO2 sloshing disturbances and Space Shuttle Program LO2 damping requirements were subsequently reduced. Analysis and sub-scale test showed the baffle count could be reduced from eight to two and still maintain margin, but a reduction to four was selected as a trade off between cost benefit and weight reduction (see Figure 11-5).

One weight saving feature of the SLWT is the removal of one more slosh baffles section, as shown in Figure 11-6. This gives a predicted performance gain of 92 pounds. This feature was incorporated into the LWT at ET-87 in 1996 to reduce weight and diminish the number of first time configuration changes for the subsequent first flight of the SLWT. Dynamics analysis showed available damping remained within requirements and propulsion and stress analysis also remained within requirements. Data are inconclusive as to whether the ET LO2 slosh baffle configuration alone caused bipod foam loss on STS-107/ET-93.

11.4.9 Possible Contributors to Strain Energy at ET Separation

The Space Shuttle Program Loads Panel is continuing to work actions to identify potential contributors to strain energy that could have led to the off-nominal yaw rate at ET separation described in Section 3.5. For induced loads during ground operations, KSC is reviewing handling and stacking (orbiter and Ground Ops). For loads that occurred during flight, Boeing GNC is looking into the left side thermal event at 300 seconds MET and if the mechanical load overcomes the joint preload during ascent. The ET project is looking into loads induced through cryogenic and pressurization cycles and the effects on the ET, such as shrinkage of the diagonal strut and overall shrinkage of the ET affecting the forward and aft attachments. The data are inconclusive as to whether potential strain energy at ET separation can be associated with events that caused bipod foam loss on STS-107/ET-93.

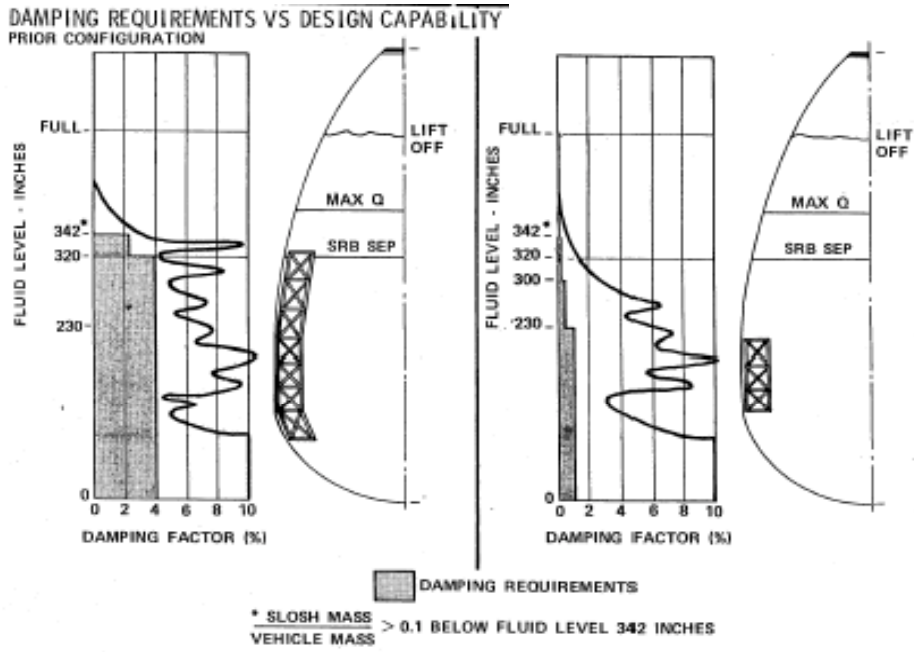


Figure 11-5. ET LO2 slosh baffle changes – ET-14

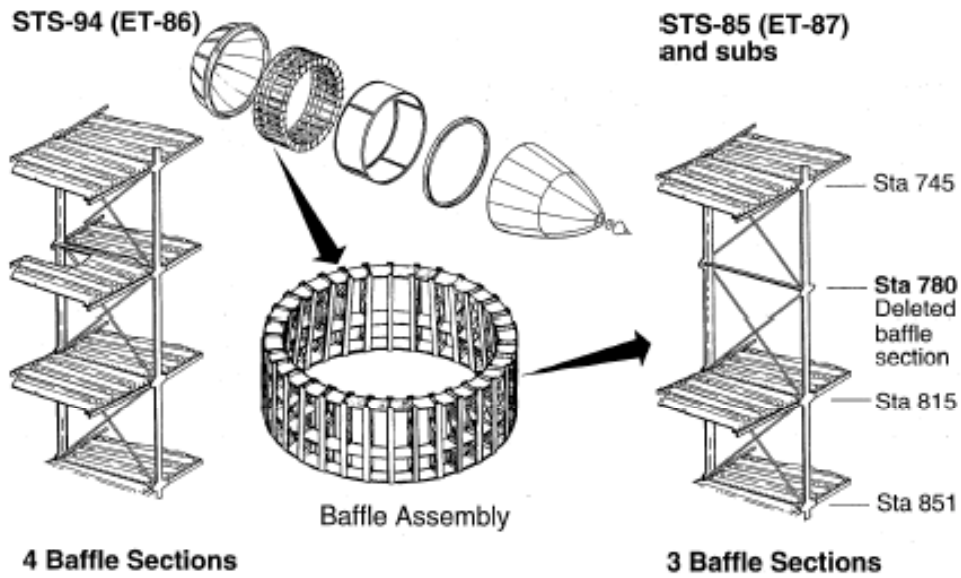
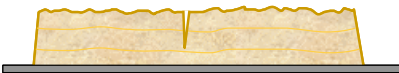

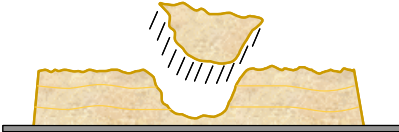



Figure 11-6. ET LO2 slosh baffle changes – ET-87

11.5 STS-107/ET-93 TPS BIPOD DEBRIS

11.5.1 Bipod Foam Failure Modes and Contributors

Four basic possible bipod failure modes have been identified (shown in Figure 11-7) and each may occur alone or act in combination with each other. However, due to lack of bipod instrumentation, it is impossible to know exactly why part of the left bipod foam came off ET-93 during STS-107 ascent. Cracking is a break in the foam, which does not exhibit material loss and is typically perpendicular to the substrate. Debond or delamination is a separation of the material running along the substrate or layer lines. A divot is a piece of material dislodged from the surface resulting in a cavity, which may or may not expose the substrate. Shear is the removal or separation of material within the cell structure and is not confined to the layer lines of the material, but is parallel to the substrate.

<u>Failure Mode</u>	<u>Primary Contributors</u>	<u>Examples</u>
Cracking	Substrate Strain Substrate bending Differential Thermal Contraction Cryopumping**	
Debond / Delamination	Differential Thermal Contraction Substrate bending	
Divot	Differential Pressure Void or cavity Cryopumping**	
Shear	Airloads	

***Cryopumping may contribute by adding to loads that induce the failure mode (but it is not a failure mode itself)*

Figure 11-7. Bipod foam failure modes

Cryopumping could contribute to bipod foam loss, shown schematically in Figure 11-8. The mechanism that drives cryopumping is the transformation of a gas to a liquid at cryogenic temperatures. Gases may condense within a void or porous material at low temperatures. Air in cavities or porous material liquefies when in contact with structure below -297°F for oxygen or -320°F for nitrogen. Pressure is reduced locally due to the condensation. If a leak path exists, more air will be “pumped,” providing more gas to condense. When the structure warms, the consequence of cryopumping is that the liquefied air returns to the gaseous state with a local pressure increase. If the leak path is large, gas escapes with no detrimental effect. However, if the leak path is small,

cracks may form in the TPS to relieve pressure, or a rapid increase in pressure may result in a divot. In order for this to occur, the inlet source must be blocked off to avoid venting out the inlet. It should be noted that testing has been unable to demonstrate cryopumping in this application.

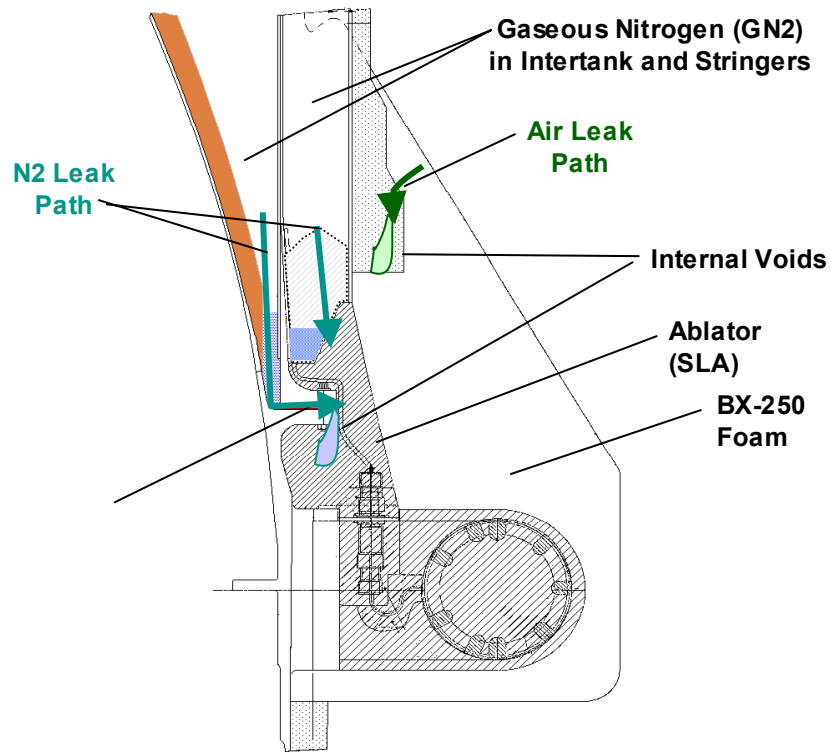


Figure 11-8. Schematic of bipod ramp - potential cryopumping

11.5.2 Test Results for Debris Assessment

Bipod TPS static and dynamic coupon tests were performed (test ET-TR-003). The objectives of these tests were to evaluate the BX-250/SLA hand-pack (HP) bond line laminate mechanical properties and investigate whether liberated BX-250 material could “pull” or “tear” SLA HP material from the bipod region. Analysis shows the critical bipod Spray-On Foam Insulation (SOFI) ramp failure mode due to direct air load is shear failure between SOFI ramp and bipod fitting substrate.

Testing shows that the potential loss of BX-250 does not liberate hand packed SLA due to impulse loading for cryogenic applications; the BX-250 fails before the SLA. For shear, testing shows BX-250 fails before SLA at all test temperatures. For tension, testing shows BX-250 fails before SLA when SLA temperatures are less than or equal to -100 °F (see Figure 11-9).

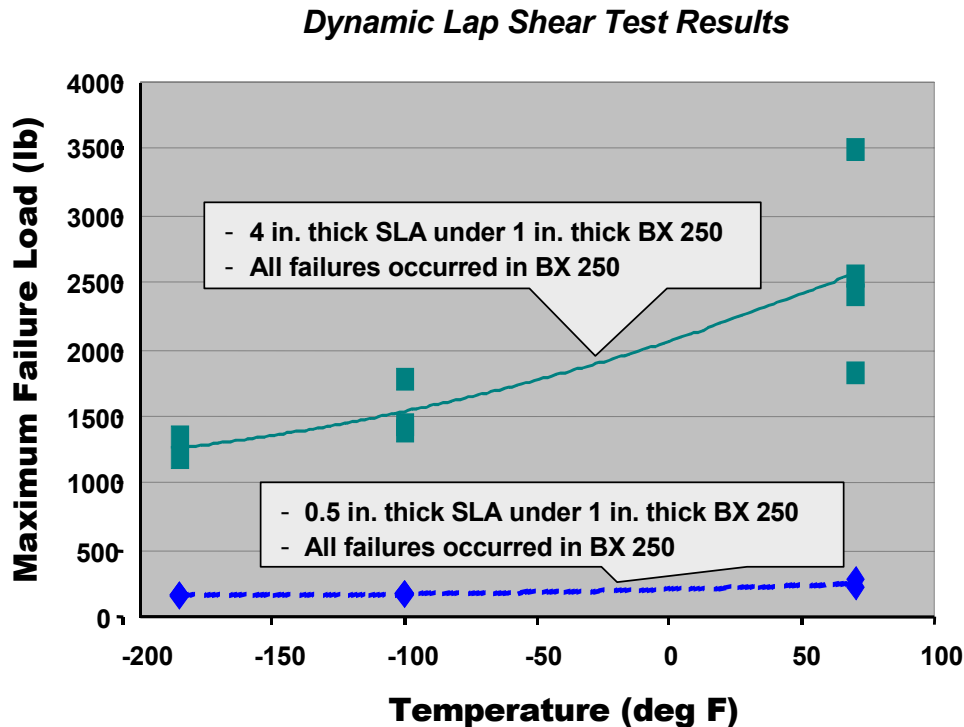


Figure 11-9. Critical test results in debris assessment

11.5.3 Max Bipod SLA Temperatures (80 seconds MET)

The maximum SLA temperatures possible at 80 seconds were analyzed to determine maximum worst-case multi-event material loss. No cryopumping or cryo ingestion was assumed in order to calculate temperatures as high as possible. STS-107 ambient environments were used. Results showed the maximum SLA temperature possible at 80 seconds MET is less than or equal to -100°F , as shown in Figure 11-10. Tension testing shows BX-250 fails before SLA at temperatures less than or equal to -100°F .

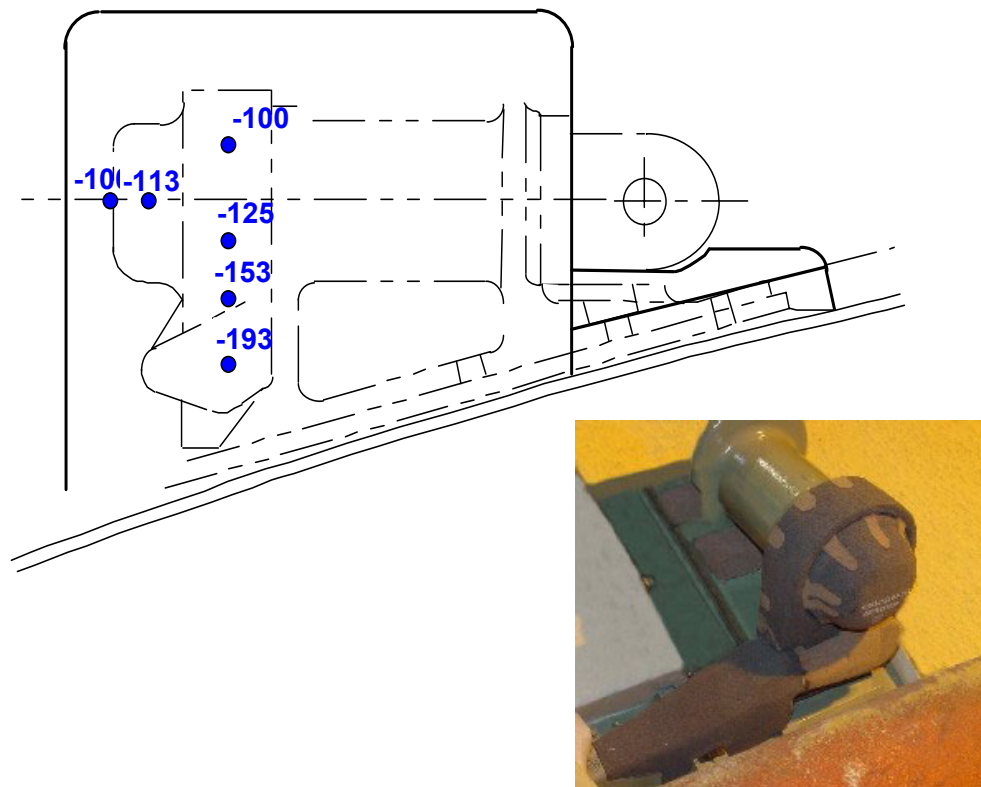


Figure 11-10. Max bipod SLA temperatures (80 seconds MET), °F.

11.5.4 Bipod Ramp As-Built Hardware Assessment

The dissection of six bipod ramps indicated similar patterns for geometry-induced defects in all ramps. Roll-overs were observed at complex substrate elements, and the majority of observations were associated with spraying over complex details at the substrate. Sporadic voids were also observed. One internal delamination and one weak plane at the knit line were observed. Critical locations, or areas at-risk for producing debris, were identified near the edge of the machined foam surface for both voids and roll-overs (see Figure 11-12). Vacuum pressure is the primary driver for divot formation; however, wind shear also contributes to flight loads. A combination of multiple large voids, geometry-induced defects, and critical locations is needed to produce significant foam loss. For example, a large interconnected void at close proximity to the surface plus a “weakened plane” (see Figure 11-13) may produce foam loss.

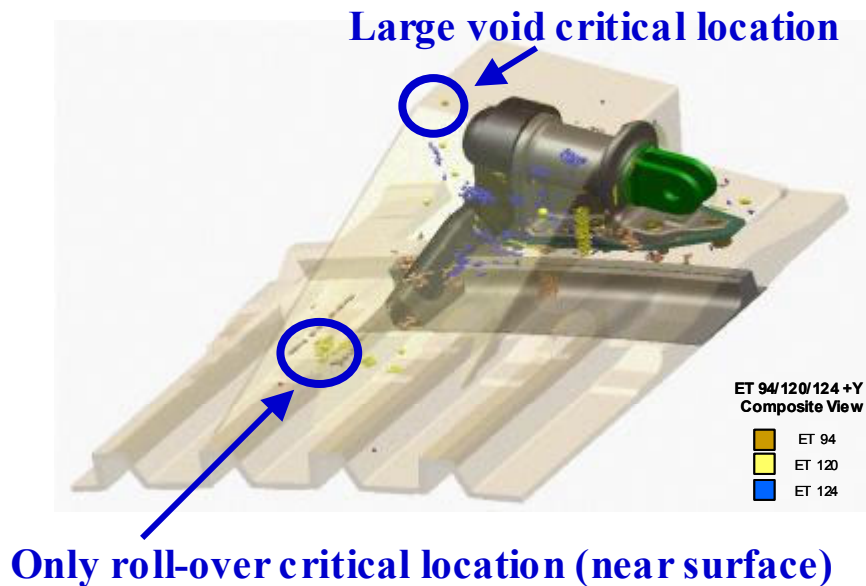


Figure 11-11. Defects found at critical locations

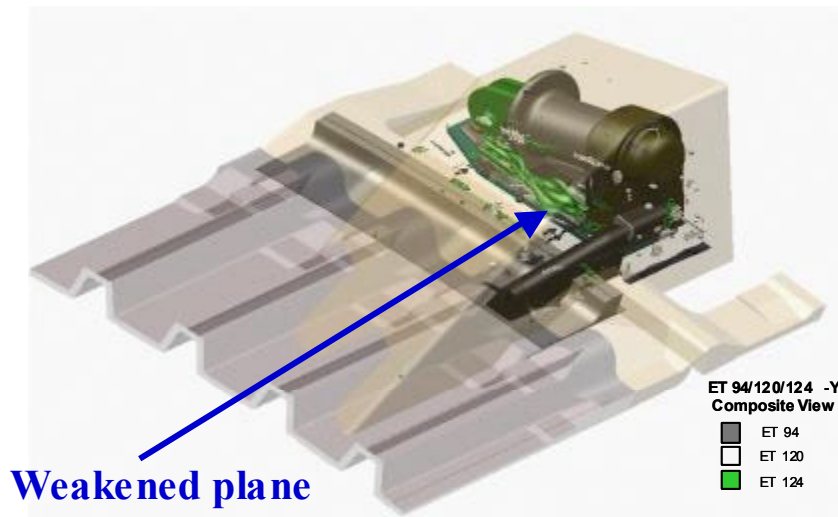


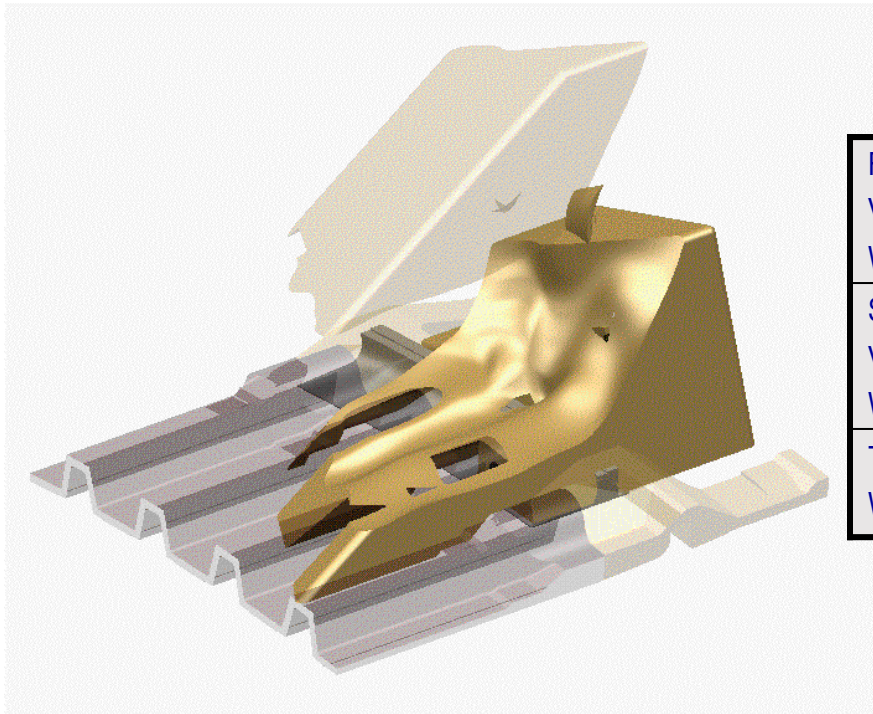
Figure 11-12. Weakened plane defect found

11.5.5 Multi-Failure Mode TPS Bipod Debris

The ET Working Group conducted an analysis coupled with test data to estimate a multi-failure mode TPS bipod debris size and weight. The ET Working Group scenario includes seven simultaneous and interactive adverse events: A large rollover occurs at the inboard stringer interface immediately below the machined foam surface, side-to-side thermal crack/weak knit line, a large void near the topmost surface one inch below machined foam surface, warm SLA environment, and foam machined to minimum tolerances (not a failure). The specific results are shown in Figure 11-13.

The determination of the STS-107/ET-93 bipod TPS debris is based on evaluation of fault tree findings, possible TPS failure modes and contributors, and results to date from TPS debris test programs including dissection, foam loss secondary effects assessment (SLA/BX-250), and bipod TPS debris size analysis. The TPS bipod debris size was determined by the ET Working Group to be approximately 870 cubic inches and 1.3 pounds.

The transport analysis presented in Section 3 suggests that the debris object may be heavier than average foam, but the ET Working Group analysis indicates there could not be ice or significant SLA in the debris and that the density of the foam is consistent. Also, the imagery analysis showed that not all the debris struck the wing, but it broke up prior to impact, with all debris passing beneath the wing, some without impacting the wing. Recall that the transport analysis presented in Section 3 states the bipod TPS debris would be 1026 cubic inches and 1.4 pounds for a 820 ft/sec velocity or 1239 cubic inches and 1.7 pounds for a 775 ft/sec velocity. The RCC foam impact test conducted at Southwest Research Institute was performed at 775 ft/sec with a 1.67-pound foam article.



Foam	
Vol.	~867.2 cu in
Weight	~1.23 lbs
SLA	
Vol.	~1.9 cu in
Weight	~0.02 lbs
TOT	
Weight	~1.3 lbs

Figure 11-13. Multi-failure mode bipod TPS debris estimated by the ET Working Group. Note that this size and weight were not used in the RCC impact testing as part of the STS-107 investigation.

12.0 SUMMARY

During the first stage of ascent, before SRB separation, the left wing of Columbia was struck by debris from the ET -Y bipod foam ramp. Analysis of the bipod foam ramp design, material, and processes suggests that the probable contributing mechanisms for foam liberation were cracks, delamination or debonding, divots, shear loads, or some combination of these. Analytical and test estimates of foam debris size, trajectory, and impact location indicate that the foam struck the left Wing Leading Edge (WLE) in the area between Reinforced Carbon-Carbon (RCC) panels 5 and 9. The impact energy tests conducted at Southwest Research Institute support the theory that the left wing RCC (lower panel 8 area, and/or an adjacent Tee seal) was damaged by the debris impact.

During ascent several new flight experience events occurred. These were all very near existing flight envelopes and well within the certified flight envelope for which the Shuttle was designed. The data indicate that all new flight experiences could be attributed to the winds aloft and SRB performance. The new flight experiences may have individually or collectively contributed to liberation of the bipod foam ramp, but data are inconclusive in this regard.

Launch radar analyses are inconclusive in determining size, shape, or identity of the debris measured after SRB separation. The radar data and analyses are inconclusive as to whether any of the debris impacted the orbiter.

There is data indicating that an object departed the orbiter on flight day 2 with a small relative separation velocity. Ballistics and Radar Cross Section (RCS) testing and analyses have excluded all tested objects except for a partial WLE Tee seal, a whole WLE Tee seal, or a partial WLE RCC panel. Data are inconclusive in determining the identity of the flight day 2 object, or whether the object was associated with the bipod foam debris impact.

Analysis of the RCC damage location and size is consistent with data from ascent. Analyses from orbiter telemetry, Modular Auxiliary Data System (MADS), aerodynamic and aero-thermal reconstruction and simulation, and debris forensics suggest that the RCC was damaged prior to Entry Interface (EI). The best estimate of the damage location is in the panel 8 lower area. Indications from modeling are that the damage size could have produced heating equivalent to a 6 to 10 inch hole diameter in the lower panel 8 area, or in one of the Tee seals adjacent to RCC panel 8.

The damage in the left wing RCC provided a pathway for hot gas to enter the left wing leading edge and support structure during entry. This resulted in significant damage to the left wing and the subsequent loss of vehicle control, leading to aerodynamic breakup.

APPENDIX A ACRONYMS AND ABBREVIATIONS

AA	Accelerometer Assembly
AC	Alternating Current
AFB	Air Force Base
AFRL	Air Force Research Labs
AFS	Air Force Station
AFSPC	Air Force Space Command
APU	Auxiliary Power Unit
BN	Ballistic Number
BSM	Booster Separation Motor
CAD	Computer-Aided Design
CAIB	Columbia Accident Investigation Board
CEI	Contract End Item
CF4	Tetraflouromethane
CFD	Computational Fluid Dynamics
CG	Center of Gravity
CSA	Canadian Space Agency
DAO	Data Assimilation Office
DAP	Digital Auto Pilot
dBsm	Decibels Relative to One Square Meter
DLR	German Aerospace Research Establishment
DOLILU	Day of Launch I-Load Update
DTA	Double Type A
EDO	Extended Duration Orbiter
EI	Entry Interface
EORF	Enhanced Orbiter Refrigerator/Freezer
ER	Eastern Range
ESA	European Space Agency
EST	Eastern Standard Time
ET	External Tank
FEP	Front End Processor
FOD	Foreign Object Debris
FRCS	Forward Reaction Control System
FREESTAR	Fast Reaction Enabling Science Technology and Research
FRSI	Felt Reusable Surface Insulation
GMT	Greenwich Mean Time
GNC	Guidance Navigation and Control

GRAM	Global Reference Atmosphere Model
GSE	Ground Support Equipment
Hi-Q	Maximum dynamic pressure
HMF	Hypergolic Maintenance Facility
HP	Hand Pack
HRSI	High-Temperature Reusable Surface Insulation
IEA	Integrated Electronics Assembly
IFA	In-Flight Anomaly
IMU	Inertial Measurement Unit
IPR	Interim Problem Report
IRN	Interface Revision Notice
ISS	International Space Station
JDMTA	Jonathan Dickinson Missile Tracking Annex
KSC	Kennedy Space Center
LAF	Lost and Found
LaRC	Langley Research Center
LCC	Launch Commit Criteria
LCD	Launch Countdown
LESS	Leading Edge Structural Subsystem
LH2	Liquid Hydrogen
LO2	Liquid Oxygen
LOS	Loss of Signal
LOX	Liquid Oxygen
LPS	Launch Processing System
LRU	Line Replaceable Unit
LWT	Light Weight Tank
MADS	Modular Auxiliary Data System
MAF	Michoud Assembly Facility
MCC	Mission Control Center
MEIDEX	Mediterranean Israeli Dust Experiment
MET	Mission Elapsed Time
MILA	Merritt Island Launch Area
MLP	Mobile Launch Platform
MMOD	Micrometeoroid or Orbital Debris
MOTR	Multiple-Object Tracking Radar
MPS	Main Propulsion System
MR	Management Review
MRB	Material Review Board
MSBLS	Microwave Scanning Beam Landing System

MSID	Measurement Stimulation Identification
NAIT	NASA Accident Investigation Team
NASA	National Aeronautical and Space Administration
NASDA	Japanese National Space Development
NDE	Non-Destructive Evaluation
NSI	NASA Standard Initiator
ODRC	Operational Data Retrieval Complex
OI	Operational Instrumentation
OMDP	Orbiter Maintenance Depot Processing
OMI	Operations and Maintenance Instruction
OMM	Orbiter Major Maintenance
OMS	Orbital Maneuvering System
PAFB	Patrick Air Force Base
PAL	Protuberance Air Load
PAPI	Precision Approach Position Indicator
PE	Performance Enhancement
PLB	Payload Bay
PMBT	Propellant Mean Bulk Temperature
PR	Problem Report
PRSD	Power Reactants Storage Device
QC	Quality Control
RCC	Reinforced Carbon-Carbon
RCS	Radar Cross Section
RDM	Research Double Module
RF	Radio Frequency
RGA	Rate Gyro Assembly
RSR	Range Separation Rate
RSRM	Re-usable Solid Rocket Motor
RSS	Range Safety System
RTV	Room Temperature Vulcanized
SAMS	Space Acceleration Measurement System
SIP	Strain Isolation Pad
SLA	Super Light Ablator
SLF	Shuttle Landing Facility
SLWT	Super Light Weight Tank
SMG	Space Meteorology Group
SOFI	Spray-On Foam Insulation
SRB	Solid Rocket Booster
SSME	Space Shuttle Main Engine

STA	Shuttle Training Aircraft
STS	Space Transportation System
TDRS	Tracking and Data Relay Satellite
TEOS	Tetraethyl Orthosilicate
TPS	Thermal Protection System
TVC	Thrust Vector Control
UHF	Ultra-High Frequency
VRCS	Vernier Reaction Control System
WLE	Wing Leading Edge